Integrated Master in Chemical Engineering

Development of a reduced-order model for oil and gas reservoirs

Master Thesis

of

Helena Isabel Monteiro Barranha

Developed in the context of the Dissertation course

carried out in

Process System Enterprise Ltd.

Supervisor at FEUP:

Dr. Alexandre Ferreira, Prof. José Miguel Loureiro

Supervisor at PSE:

Dr. Adekola Lawal

Department of Chemical Engineering

July 2015

"Science is a delight; evolution has arranged that we take pleasure in understanding – those who understand are more likely to survive."

- Carl Sagan, in *Cosmos*

Acknowledgements

First of all I would like to thank my family for all the support, not just through this stage, but during my whole life as a student. Most importantly, I have to mention my parents who have always encouraged me to be a better student and a better person.

I want to acknowledge Dr. Adekola Lawal, Dr. Alexandre Ferreira and Prof. José Miguel Loureiro for the support and contribution to this project, and Prof. Costas Pantelides for this opportunity, in such a great and welcoming company, and for the financial support.

To my “neighbours”, Mariana Gomes and Ana Morgado, I want to show my appreciation for encourage me to accept this challenge, and for accompanying me in this path.

I want to thank all my professors at FEUP for all that they have taught me, and especially Prof.Luís Miguel Madeira for providing such great opportunities for academic internships.

Last but not least I would like to mention all my friends at FEUP, who made the last five year become unforgettable.

Resumo

Este projeto consiste no trabalho desenvolvido no âmbito da unidade curricular Dissertação, durante a realização de um estágio académico na *Process System Enterprise Limited*, no contexto de modelação de reservatórios de petróleo na área de captura e armazenamento de carbono.

Este estudo é motivado pela importância da previsão do comportamento de reservatórios na produção de petróleo e na avaliação da sua propensão para armazenamento de dióxido de carbono.

Neste relatório é realizada uma revisão das mais importantes propriedades do reservatório e dos fluídos nele contidos. Quanto ao reservatório são também analisados e avaliados os diferentes tipos de produção, tendo por base a recuperação de petróleo.

A análise nodal é apresentada como o tipo de modelo utilizado e é feita uma descrição detalhada da fase de modulação, na qual são explicadas as equações implementadas. Seguidamente, são utilizados dois casos de estudo para validação e análise de sensibilidade do modelo.

Após a execução de simulações, foi possível concluir que apesar das simplificações aplicadas, o modelo e capaz de prever corretamente o comportamento de um reservatório com mecanismo de gás em solução. Contudo, a baixas pressões o desempenho do reservatório não é bem descrito devido a grande quantidade de gás que torna o reservatório mais semelhante a um reservatório de gás.

Palavras-chave: reservatório de petróleo, análise nodal, mecanismo de gás em solução, modulação.

Abstract

This project consists on the work developed in the Dissertation course during an academic internship at Process System Enterprise Ltd, in the context of reservoir modelling within the carbon capture and storage (CCS) field.

The motivation for this study was the importance of predicting reservoir's performance on the oil production side and on evaluating the reservoir's propensity to injection of carbon dioxide.

This monography comprises a review on reservoir and fluids' most important properties and, on the reservoir side, the types of drive mechanisms are analysed and evaluated, based on the ultimate oil recovery.

Then Nodal Analysis was chosen as the model-type and a full description of the modelling stage is made, in which the model equations are explained. Subsequently, two case studies are used to the model's validation and sensitivity analysis.

From the simulations executed, it was possible to conclude that despite the simplifications applied, the model is capable of correctly predict the behaviour of a solution-gas drive reservoir. However, at low reservoir pressures the reservoir's performance is not well described as the high amount of gas present makes it similar to a gas reservoir.

Keywords: oil reservoir, nodal analysis, solution-gas drive, modelling.

Declaração

Declara, sob compromisso de honra, que este trabalho é original e que todas as contribuições não originais foram devidamente referenciadas com identificação da fonte.

Helena Isabel Monteiro Barranha

06/07/2015

Contents

List of Figures

List of Tables

Nomenclature

A	Area	ft^2
B	Formation volume factor	bbl/stb ; scf/stb
c	Compressibility	$psia^{-1}$
c_p	Pore compressibility	$psia^{-1}$
D	Well diameter	ft
f	Friction factor	
G	Cumulative evolved gas	scf
g	Gravity acceleration	ft/s^2
g_c	Gravitational conversion factor	$lbm.ft/(lbf.s^2)$
h	Thickness	ft
k	Absolute Permeability	mD
k_r	Relative permeability	
L	Length	ft
M	Mobility ratio	
M_g	Apparent gas molecular weight	
n	Number of moles	mole
N	Cumulative production	ft^3
ΔN	Volume of oil reduction	ft^3
$OOIP$	Original oil in place	stb
p	Pressure	psia
p_{nw}	Pressure of the non-wetting fluid	psia
$\overline{p_R}$	Average reservoir pressure	psia
p_w	Pressure of the wetting fluid	psia
p_{wf}	Wellbore flowing pressure	psia
P_c	Capillary pressure	psia
Δp	Pressure difference	psia
Δp_f	Friction losses	psia
Δp_g	Gravitational losses	psia
q	Production flow rate	stb/d ; scf/d
R	Ideal gas constant	$ft^3.psi/(^oR.lb\text{-}mol)$
r	Radius	ft
r_a	Aquifer radius	ft
r_e	Drainage area radius	ft
R_s	Dissolved-gas oil ratio	scf/stb
R_{sw}	Gas-water solubility	scf/stb
r_w	Radius of the well	ft
S	Saturation	
S_c	Critical saturation	
S_{om}	Movable oil saturation	
S_{wirr}	Irreducible water saturation	
T	Temperature	^oF
v	Velocity	ft/s
V	Volume	ft^3
V_p	Pore volume	ft^3
z	Gas compressibility factor	

Subscripts

bp	Bubble-point
f	Formation
g	Gas
go	Dissolved gas in the oil
i	Initial
$node$	Node
o	Oil
s	Standard conditions
sep	Separator conditions
t	Total
w	Water
wf	Well flowing conditions

Greek letters

γ	Specific gravity	
θ	Contact angle	
λ	Mobility	mD/cP
μ	Viscosity	cP
ρ	density	lb/ft^3
σ	Tension	Dynes/cm
ϕ	Porosity	

Acronyms

CCS	Carbon capture and storage
EOR	Enhanced oil recovery
IPR	Inflow performance relationship
PSE	Process System Enterprise

1 Introduction

Petroleum occurs throughout the earth in different forms, as gas, liquid or solid. It consists essentially on a mixture of hydrocarbon compounds that can also contain slight amounts of nitrogen, oxygen and sulphur compounds (Barker et al. 2005, Levorsen 1956).

While organic matter is buried in sediments, in a reducing environment, and subjected to increasing temperature and pressure, petroleum is created as an intermediate in a transformation process that ultimately leads to methane and graphite (Barker et al. 2005).

The processes involved in petroleum generation in the source rock are the migration out of that rock and to the reservoir, maturation and alteration which operate to change the composition of the petroleum, after it has accumulated in the reservoir (Barker et al. 2005).

Buoyancy is the leading driving force in oil accumulation. Being lighter than water, oil rises and is concentrated in the highest part of the container. In order to prevent its escape, the upper contact of the porous rock with impermeable cover must be concave. Such a container is called a trap, and the portion of the trap that holds the oil is called reservoir. Many traps result from complex combinations of structural and stratigraphic variations (Barker et al. 2005, Levorsen 1956).

Because of its association with rocks, petroleum is considered one of the “mineral resources” and is commonly called mineral fuel. When in the liquid phase it is entitled crude oil (Levorsen 1956).

The “black oil” fluid in the reservoir consists of oil with or without a gas phase which can be partially dissolved in the oil depending on the reservoir temperature and pressure. The type of reservoir also depends on whether water is present in the reservoir (Reinicke et al. 2014, David Martin and Colpitts 1996).

Petroleum’s commercial importance became apparent after the middle of the nineteenth century when it was first discovered in large quantities underground, creating interest around its origin (Levorsen 1956).

The development of reservoir models is a very important matter to avoid excessive spending on reservoir exploitation.

1.1 Motivation and Objective

Process System Enterprise Ltd (PSE) is the world's leading purveyor of Advanced Process Modelling technology and related model-based engineering services to process industries. The gPROMS® platform, provided by PSE, enables the costumers to reduce uncertainty and make better, faster and safer design and operating decisions concerning their processes (PSE).

gCCS, the first full-chain modelling software for carbon capture and storage (CCS), was first launched on July 9th 2014, and on July 31st of the same year it was announced that it would be part of the Shell Peterhead CCS project. This modelling tool contains steady-state and dynamic models of all major CCS operations such as power generation, compression, capture and injection (PSE 2014b, a).

The reservoir plays an important role in the carbon storage, when enhanced oil recovery (EOR) by injection of carbon dioxide is considered. Hence, modelling the reservoir's performance can help evaluate both its production capacity and propensity for EOR.

1.2 Structure of the thesis

Chapter 2 reviews the reservoir and fluids' properties which are crucial to oil and gas production's estimation such as density, viscosity and permeability. In addition, the different types of drive mechanisms during primary recovery are presented, and this recovery stage is differentiated from enhanced oil recovery.

The materials and methods section, chapter 3, presents the gPROMS® ModelBuilder platform which was used to develop the reservoir model.

In chapter 4 the Nodal analysis method is introduced, and it is explained how it was implemented in gPROMS®. In the same section all the equations and correlations used for modelling the reservoir are discretized.

The model validation is described in chapter 5. Two case studies were performed, one idealized reservoir and the Lousiana volatile-oil reservoir, in order to validate the equations implemented. As part of the validation procedure, it is also made the discussion of the results for each case.

The final main chapter contains the conclusions of this study and the future work.

In the appendix sections, the full data from the case studies' reservoirs and supplementary results from the simulations are shown.

2 Background

2.1 Reservoirs' Fluids Properties

The physical properties and crude oils' compositions vary extensively with the location of the reservoir and the stage of oil production (Hocking 2005).

The key fluid properties that require special attention are the formation volume factors B, which are given by the ratio of the fluid's volume at reservoir conditions to a unit volume at the surface; the bubble-point pressure p_{bp}; the dissolved-gas oil ratio R_s; the viscosity μ; the surface and in situ densities ρ and compressibility c.

The gas properties are calculated by equation 2-1, which is the real-gas equation with a gas deviation factor z that accounts for non-ideal behaviour. This factor needs to be estimated as a function of reservoir temperature and pressure and this dependence is showed in Fig. 2-1 (Reinicke et al. 2014, Craft and Hawkins 1991, David Martin and Colpitts 1996).

$$PV = znRT \tag{2-1}$$

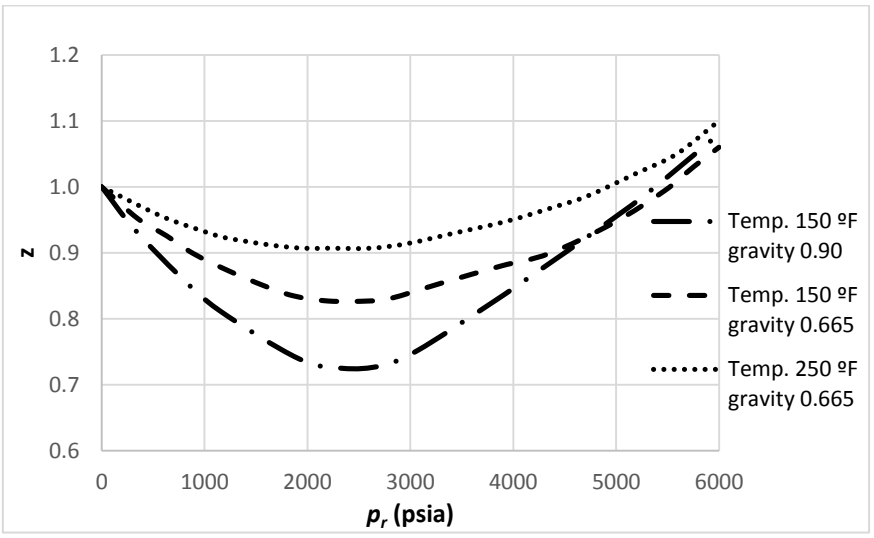

Fig. 2-1 - Effect of temperature, pressure and composition on the gas deviation factor (Craft and Hawkins 1991).

2.2 Properties of fluid-containing rocks

Rock properties are determined by laboratory analysis on cores from the reservoir. The cores are removed from the reservoir environment, which induces changes in the core bulk volume, pore volume, reservoir fluid saturations and, sometimes, formation wettability.

The effect of these changes on rock properties may range from negligible to substantial, depending on the characteristics of the formation and property of interest.

The main properties are porosity, permeability, saturation, overburden pressure, capillary pressure, wettability, surface and interfacial tension. These property data are essential for reservoir engineering calculations as they directly affect both the quantity and the distribution of hydrocarbons and, when combined with fluid properties, control the flow existing phases within the reservoir (Ahmed 2006).

2.2.1 Porosity

The porosity of a rock ϕ is a measure of the storage capacity that is capable of holding fluids. It must be estimated for the entire reservoir and it is affected by compactness, character and amount of cementation, shape and arrangement of grains and by uniformity of grain size and distribution (Reinicke et al. 2014, David Martin and Colpitts 1996).

As sediments were deposited during rocks' formation, some void spaces developed became isolated from the others by excessive cementation. This result on the existence of two distinct types of porosity: absolute and effective porosity (Ahmed 2006, David Martin and Colpitts 1996).

The absolute porosity is defined as the ratio of the total pore space in the rock to that of the bulk volume. A reservoir may have high porosity but it might not be accessible to fluids' flow for lack of pore interconnection.

The effective porosity, used in all reservoir engineering calculations, represents the interconnected pore space that contains the recoverable hydrocarbon fluids (Ahmed 2006).

The reservoir rock may generally show large variations in porosity vertically but does not show significant variations in porosity parallel to the bedding planes. Porosity of oil-bearing sandstones is 15% to 30%, and it is higher than limestones and dolomites' porosity (0 to 20%) (Ahmed 2006, Reinicke et al. 2014, David Martin and Colpitts 1996).

2.2.2 Permeability

The permeability, k, is expressed in units of Darcy and represents a resistance to flow caused by the tortuosity of the pore network. It is given by the Darcy equation for the flow rate, which is represented in equation 2-2, where q is the flow rate, Δp is the pressure

difference, L is the length and A is the area, μ has the same meaning as previously mentioned.

$$k = \frac{q\mu L}{A\Delta p} \tag{2-2}$$

The rock permeability controls the directional movement and the flow rate of the reservoir fluids in the formation (Ahmed 2006, Reinicke et al. 2014).

An adequate knowledge of permeability distribution is critical due to the prediction of reservoir depletion by any recovery process. It is rare to encounter a homogeneous reservoir in actual practice. In many cases, the reservoir contains distinct layers, blocks, or concentric rings of varying permeability.

Where smaller-scale heterogeneities exist, permeability must be averaged depending on how its values are distributed in the reservoir (David Martin and Colpitts 1996).

2.2.3 Rock compressibility

A reservoir, situated thousands of feet underground, is under an overburden pressure triggered by the weight of the overlying formations. Overburden pressures vary with region depending on factors such as depth, nature of structure, consolidation of the formation, and possibly the geologic age and history of the rocks. However, depth of the formation is the most important factor to consider (Ahmed 2006).

The compressible force (pressure) applied to the reservoir by the weight of the overburden does not approach the overburden pressure. The difference between overburden and internal pore pressure is called effective overburden pressure.

Throughout the pressure depletion processes, the internal pore pressure decreases, and so effective overburden pressure increases causing the reduction of the bulk volume of the reservoir, and expansion of the sand grains within pore spaces (Ahmed 2006).

These two volume changes tend to reduce the pore space and, therefore, the porosity of the rock. Compressibility typically decreases with increasing porosity and effective overburden pressure (Ahmed 2006, Reinicke et al. 2014).

For most petroleum reservoirs, the rock and bulk compressibility are considered small when compared with the pore compressibility, c_p. Accordingly, the common term used to describe the total compressibility is the formation compressibility c_f and it is set equal to c_p. In general, the formation compressibility is the same order of magnitude as the

compressibility of the oil and water and, therefore, cannot be regulated (Ahmed 2006, David Martin and Colpitts 1996).

2.2.4 Saturation

Saturation is defined as the fraction of pore volume that a particular fluid occupies. The densities of the fluids define the way fluids are separated, i.e. oil overlain by gas and underlain by water. Connate or interstitial water also exists throughout the oil and gas, as it is retained by forces, called capillary forces because they are only significant in pore spaces of capillary size.

Critical saturation S_c is what the fluids must exceed to flow, and at this particular saturation it does not flow. After the displacement operation of the oil from the pores by water or gas injection, the remaining oil is characterized by the residual oil saturation.

According to the previous types of saturation, movable saturation S_{om} can be defined as the fraction of pore volume occupied by movable oil, given by equation 2-3, in which S_{wc} and S_{oc} are the critical saturations of water and oil, respectively (Ahmed 2006).

$$S_{om} = 1 - S_{wc} - S_{oc} \tag{2-3}$$

2.2.5 Wettability

Wettability is the tendency of one fluid to adhere to a solid surface in the presence of other immiscible fluids. This property is expressed by measuring the angle of contact at the liquid-solid surface. This angle, termed contact angle θ, is always measured through the liquid to the solid (see Fig. 2-2).

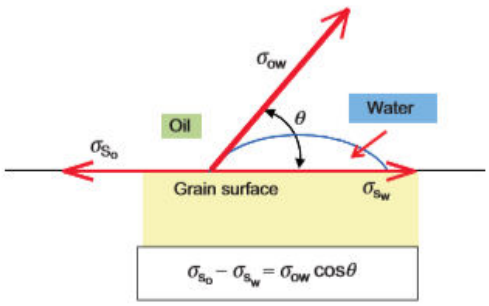

Fig. 2-2 - Rock wettability (Reinicke et al. 2014).

Surface and interfacial tensions σ are the surface free energy resulting from molecular interactions, which affects the capillary pressure. When temperature increases or dissolved gas is present, surface tension of crude oil decreases (Reinicke et al. 2014, David Martin and Colpitts 1996).

2.2.6 Capillary Pressure

The capillary forces result from the combined effect of the surface and interfacial tensions of the rock and fluids, the pore size and geometry, and the wetting characteristics of the system (Ahmed 2006).

When two immiscible fluids are in contact, a discontinuity in pressure appears between the two fluids, which depends upon the curvature of the interface separating the fluids. This pressure difference is the capillary pressure P_c and it is expressed by equation 2-4 where the subscripts nw and w are for the non-wetting and wetting phases, respectively (Ahmed 2006, Reinicke et al. 2014, David Martin and Colpitts 1996).

$$P_c = p_{nw} - p_w \tag{2-4}$$

In order to uphold a porous medium partially saturated with non-wetting fluid and while in presence of the wetting fluid, maintaining the pressure of the non-wetting fluid at a value greater than that in the wetting fluid is essential. That is, the pressure excess in the non-wetting fluid is the capillary pressure, and this quantity is a function of saturation (Ahmed 2006, Reinicke et al. 2014).

2.3 Flow geometries

Although the real path of the fluids in the porous medium is irregular, the average paths may be represented by three flow geometries: linear, radial and spherical, from which the first two have the greatest practical interest (see Fig. 2-3).

The linear flow consists on parallel flow lines, in a cross section with constant flow. In the radial flow, straight flow lines converge toward the centre which represents the well. Finally, the spherical flow is represented by straight flow lines that converge toward a common centre in three dimensions (Craft and Hawkins 1991).

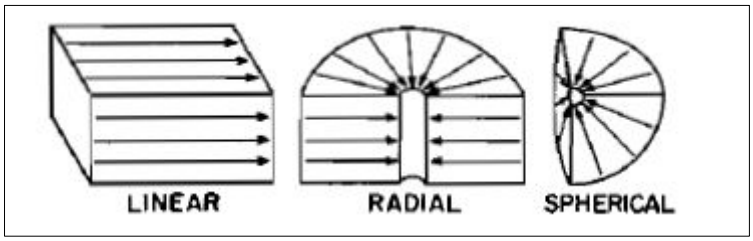

Fig. 2-3 - Illustration of the three flow geometries (Craft and Hawkins 1991).

2.4 Primary Recovery

The first fraction of crude oil is recovered from the reservoir by fluids expansion, as it is trapped under pressure in the rock. When pressure starts to drop, the oil's movement through the wellbore decreases requiring the installation of pumps to lift the oil to the surface (Craft and Hawkins 1991, David Martin and Colpitts 1996).

As production continues, pressure declines and it is required that a fluid enters the reservoir to maintain pressure. The amount of oil that can be produced by the natural reservoir energy depends on the reservoir type which can be water-drive, solution-gas drive, gas-cap drive or gravity drainage drive reservoir (Ahmed 2006, Reinicke et al. 2014, David Martin and Colpitts 1996, Craft and Hawkins 1991).

2.4.1 Water-drive reservoir

In this type of reservoir there is a connection between the oil and a porous, water saturated rock called aquifer. It is the pressure caused by this compressed water that forces the oil to the surface. Fig. 2-4 shows a sketch of an idealized system of a reservoir and an edge aquifer (Craft and Hawkins 1991, Ahmed 2006).

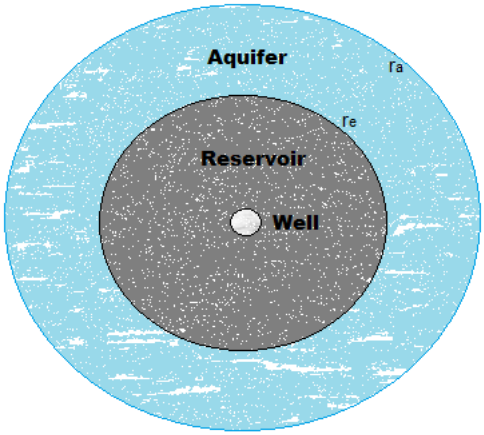

Fig. 2-4 - Top view of an idealized reservoir and an edge aquifer (Sureshjani and Gerami 2011).

As pressure is reduced gradually during oil and gas production, a natural water-flood is created, displacing the oil in the reservoir almost volume by volume.

This natural displacement maintains pressure, stopping gas from evolving from solution. As a result, the producing gas-oil ratio suffers little change, particularly if there is no free gas initially present in the reservoir.

The ultimate oil recovery achieved in this type of reservoir is usually much larger than under any other mechanisms. However, it depends upon the encroachment efficiency of the water, which decreases with the heterogeneity increase of the rock, because of the unevenly spreading of the water (Ahmed 2006, Sureshjani and Gerami 2011, Reinicke et al. 2014, Craft and Hawkins 1991).

The ultimate oil recovery ranges from 35% to 75% of the original oil in place (Ahmed 2006).

2.4.2 Solution-gas reservoir

Crude oil under high pressure can contain a significant amount of dissolved gas. When oil is produced, pressure in the reservoir decreases and in some regions it can drop below the bubble-point pressure, which leads to gas escape (Craft and Hawkins 1991).

In this type of reservoir the pressure drops rapidly and continuously as there are no extraneous fluids or gas caps to displace the oil removed until the bubble point is reached.

When the reservoir pressure reaches the bubble point, the gas evolves from solution throughout the reservoir, and once the critical gas saturation is exceeded, the free gas flows towards the wellbore and gas-oil ratio increases.

The formation of gas saturation along the reservoir contributes for this type of drive mechanism to be the least efficient method when it comes to ultimate recovery. It can vary from 5% to about 30% (Ahmed 2006, Craft and Hawkins 1991).

2.4.3 Gas-cap drive reservoir

The displacement of oil is due to the expansion of compressed gas on the top of the reservoir called gas-cap, when pressure decreases during oil production (see Fig. 2-5).

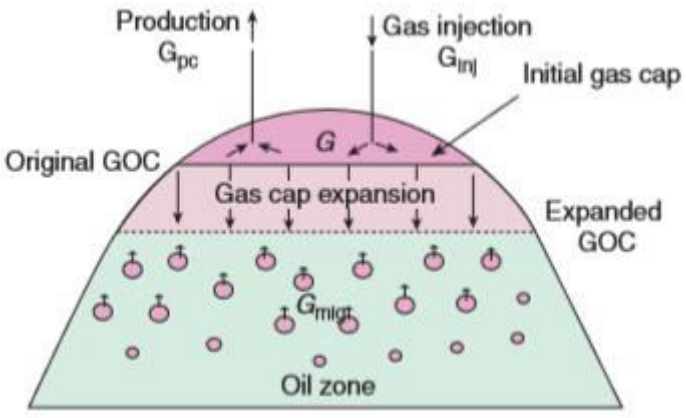

Fig. 2-5 - Gas-cap expansion (Reinicke et al. 2014).

The reservoir pressure decreases slowly, tending to being maintained higher than in a solution-gas drive reservoir. The degree at which pressure can be maintained depends on the volume of the gas cap compared to the oil in the reservoir.

The pressure wave from the gas cap expansion, combined with the fact that no gas saturation is being formed makes this type of drive achieve a recovery that ranges from 20% to 40% (Ahmed 2006, Reinicke et al. 2014).

2.4.4 Gravity drainage drive reservoir

This drive mechanism is a result of differences in densities of the fluids in the reservoir. The action of the gravitational forces in the fluids determines the relative positions of fluids: gas on top, oil underlying the gas, and water underlying the oil.

During the long periods of time of petroleum accumulation and migration processes, it is assumed that the reservoir fluids are in equilibrium, which means that gas-oil and oil-water interfaces are essentially horizontal (Ahmed 2006).

Gravity drainage of fluids is present in all reservoirs, but it may have larger contribution to oil production in some reservoirs.

The rate of pressure decline on this type of mechanism depends mainly upon the amount of gas conservation. If the reservoir operates only under drainage drive, pressure will decline rapidly.

The evolved gas migrates to the top of the field due to gravitational segregation of the fluids, which leads to low gas-oil ratio when producing from low wells. On the other hand, high wells will involve increasing gas-oil ratio.

Ultimate recovery will vary widely, depending on the extent of depletion of gravity drainage alone. In this type of reservoir it is important that the oil saturation near the well is maintained as high as possible, because high oil saturation means a higher oil flowrate and lower gas flowrate.

Gravity drainage mechanism is best exploit if the wells are located as low as possible to avoid any gas near the well. Also, permeability, oil viscosity, and producing rates are major factors affecting the ultimate recovery (Ahmed 2006).

2.5 Secondary and Enhanced Oil Recoveries

When the rate of oil production declines, it can be increased by injecting secondary energy as gas or water, in order to maintain pressure in the reservoir.

The injection of water is in some cases designed to disposal of brine water or to implement a water-drive, after primary recovery. If permeability is too low, gas injection is preferred as the rate of water injection may be low (Reinicke et al. 2014).

The enhanced oil recovery (EOR) processes are the techniques which allow a higher recovery than primary or secondary recovery. These techniques include miscible processes, chemical oil flooding, thermal recovery and microbial processes (Reinicke et al. 2014, David Martin and Colpitts 1996).

2.5.1 Mobility control

The mobility of any fluid, λ, is given by equation 2-5, which represents the ratio of the fluid's permeability to its viscosity.

$$\lambda = \frac{k}{\mu} \tag{2-5}$$

The mobility ratio M is calculated by equation 2-6.

$$M = \frac{\lambda_{displacing\ fluid}}{\lambda_{displaced\ fluid}} \tag{2-6}$$

To improve the displacement efficiency, the mobility ratio should be reduced to one or less, which is called mobility control (Ahmed 2006, Dake 1978, Sureshjani and Gerami 2011).

2.5.2 Water flooding

Water flooding is the most common method of secondary recovery, but before undertaking this process it is necessary to consider factors such as reservoir geometry and depth, fluids and rock properties and fluid saturations (Ahmed 2006).

As the oil is moving in head from the injected water front, its permeability must be evaluated at the initial water saturation.

The water's mobility before breakthrough will be constant, as water permeability is characterized by average water saturation. After breakthrough, the water average saturation increases, which increases the mobility ratio (Ahmed 2006, Dake 1978).

The determination of the optimum time to water-flood is based on oil recovery prediction, production flowrates and on the costs of maintenance and monetary investment (Ahmed 2006).

2.5.3 Carbon dioxide flooding

Carbon dioxide, CO_2, is injected in the reservoir as gas, and its high solubility in oil has favourable effects on oil recovery. When CO_2 is dissolved, oil saturation increases above the residual saturation, increasing oil's permeability. Also, oil's viscosity is reduced, improving the mobility control (Ahmed 2006, Dake 1978).

This type of enhanced oil recovery also enables the CO_2 storage, for which it is required that the reservoir is situated at depths below 800 m, where it is in a liquid or supercritical state.

Once injected in the reservoir, the fraction of CO_2 retained depends on physical and geochemical trapping mechanisms, such as an impermeable layer ("cap rock"), and capillary forces, respectively (Metz et al. 2005).

3 Materials and Methods

3.1 gPROMS® ModelBuilder

gPROMS® ModelBuilder 4.1.0 was the platform used to develop the reservoir model. This advanced modelling and flowsheeting tool is the heart of the gPROMS® products (see Fig. 3-1).

ModelBuilder is used to build, validate and execute steady-state and dynamic process models of any complexity. It combines industry-leading custom modelling competences with a process flowsheeting environment, to offer the process industries the most powerful advanced process modelling tool (PSE).

The conception of a new model entity enables the user to write the model equation in the language tab, build the input window, by defining the required inputs in the interface language tab, and select the icon of the model in the interface tab.

For this project, after the implementation of the equations, a Process Entity was created for each simulation to define how it should be performed. The simulations can be executed for a chosen period of time, or it can be selected a condition which will determine the end of the simulation. This is defined on the Schedule tab of the Process.

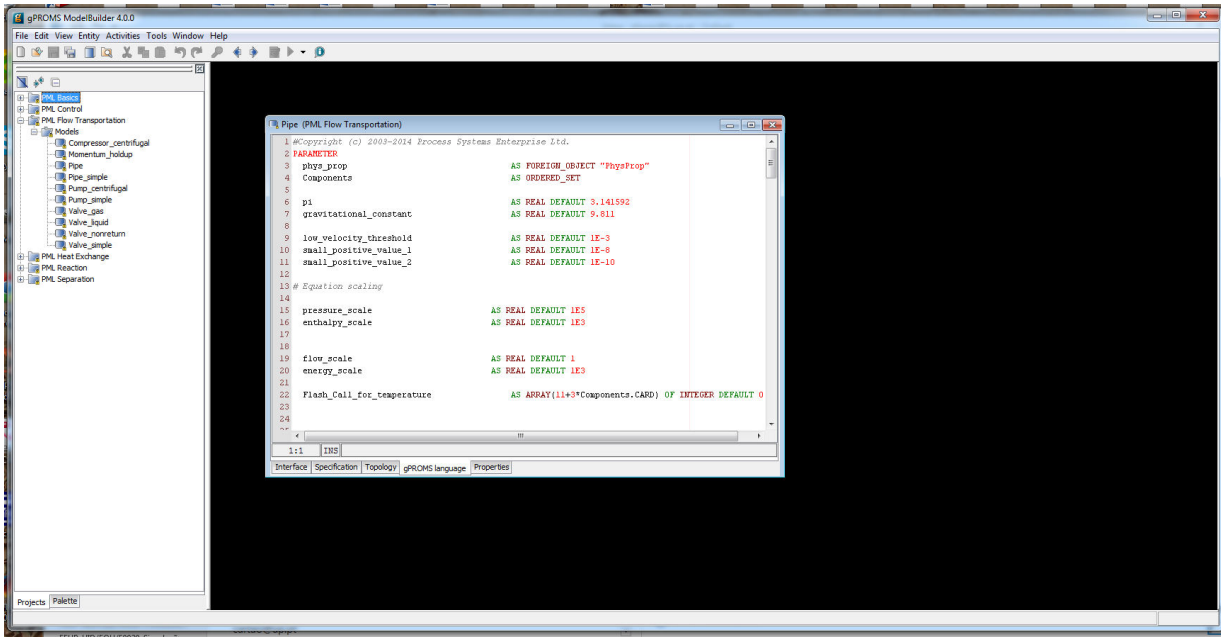

Fig. 3-1 - gPROMS ModelBuilder appearance.

4 Mathematical Description

4.1 Nodal Analysis

The nodal analysis procedure consists of selecting a division point in the producing well and dividing the system into a reservoir dominated component and a piping system component.

All the components upstream of the node compromise the inflow section (reservoir), while all of the components downstream influence the outflow section (pipes).

The method's implementation requires that the flow into the node equals the flow out of the node, and that only one pressure exists at the node (Beggs 2003).

The pressure drop in the reservoir varies with flowrate, and if the node's pressure p_{node} is plotted against oil flowrate q_o, two curves will be produced, i.e. one for each section, which result from the pressure losses in the respective component. The intersection of the two curves will give the conditions that satisfy the requirements of the method (see Fig. 4-1).

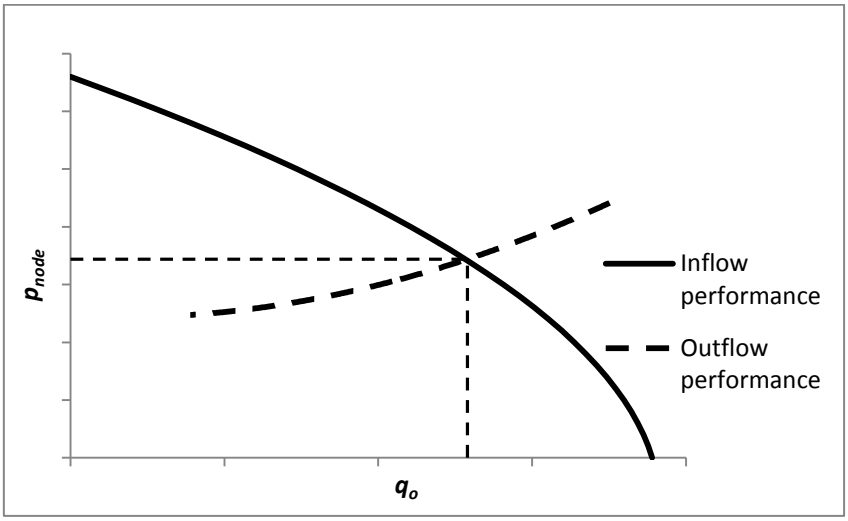

Fig. 4-1 - Nodal analysis plot (Beggs 2003).

At a particular time of the systems' life, two pressures are fixed, i.e. they are not a function of the production flowrate. These pressures are the reservoir average pressure and the system's outlet pressure which usually is the separator pressure. However, if either pressure suffers changes, the curves will change, and the intersection will be shifted. This leads to a new flowrate and a new node's pressure (Beggs 2003).

4.1.1 Reservoir: Solution-gas drive modelling

This model considers the node at the bottom hole of the production well, and the separator pressure as the outlet pressure of the whole system.

As oil is produced, the average reservoir pressure decreases, but it is also important to analyse the pressure profile inside the reservoir. Equation 4-1 relates the pressure inside the reservoir with the radius r, and a typical pressure profile is shown in Fig. 4-2 (Reinicke et al. 2014).

$$p(r) - p_{wf} = \frac{141.2 q_o \mu_o B_o}{k_o h} \ln\left(\frac{r}{r_w}\right) \tag{4-1}$$

Where p is the pressure at radius r, p_{wf} is the wellbore flowing pressure, h is the reservoir thickness, and r_w the radius of the well. This profile considers radial and horizontal flow of oil.

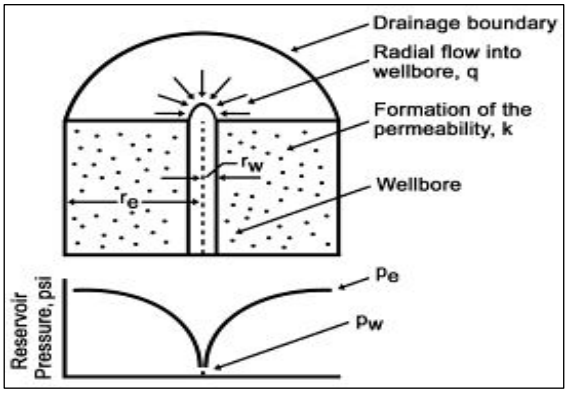

Fig. 4-2 – Illustration of a reservoir and its pressure profile.

The pressure inside the reservoir decreases as it gets near the production well, and during oil production the pressure profile is altered because of the drop in the average reservoir pressure. This alteration in the pressure profile is illustrated in Fig. 4-3.

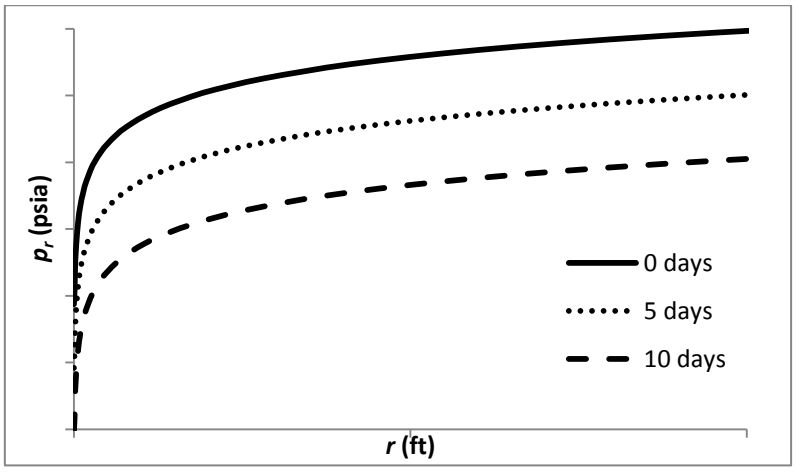

Fig. 4-3 – Reservoir's pressure profile at different production times.

The inflow performance relationship (IPR), which relates the wellbore flowing pressure with the average reservoir pressure $\overline{p_R}$ to obtain the oil flowrate, is represented by Darcy's law (equation 4-2) (Chen 2007, Beggs 2003).

$$q_o = \frac{k_o h(\overline{p_R} - p_{wf})}{\mu_o B_o[ln(r_e/r_w) - 0.75]} \tag{4-2}$$

Where r_e is the radius of the drainage area of the reservoir.

The IPR curve is affected by the changes in oil properties as relative permeability and viscosity. Moreover, it is important to consider gas evolving from solution if pressure drops below the bubble point pressure.

Both equation 4-1 and equation 4-2 are obtained from Darcy's law, but the first one was rearranged to calculate pressure, while the second is used to calculate the flowrate, based on the pressures at the end and beginning of the system. The combination of the two ways of writing the same equation allows to model oil's behaviour inside the reservoir, assuming a constant production flowrate flowing in the reservoir and entering the well.

The presence of water, when above its irreducible saturation will also affect the production flowrate, which will now contain water, and consequently the pressure profile will be changed.

The water flowrate is expressed by equation 4-3, and the reservoir pressure profile will be, in this case, written as a function of the total flowrate and of the two fluids' properties (Craft and Hawkins 1991).

$$q_w = \frac{k_w h(\overline{p_R} - p_{wf})}{\mu_w B_w[ln(r_e/r_w) - 0.75]} \tag{4-3}$$

As water and oil are produced, both quantities will be important to evaluate the decrease in average reservoir pressure. Equation 4-4 relates the initial average reservoir pressure $\overline{p_{R_i}}$ with the cumulative productions of oil N_o and water N_w (Ahmed 2006).

$$\overline{p_R} = \overline{p_{R_i}} - \frac{N_o + N_w}{c_t \phi V} \tag{4-4}$$

The cumulative productions are calculated by establishing that their derivatives are equal to the flowrate of the correspondent fluid.

Production of fluids leads to pressure drop, and consequently to a decrease in total flowrate as seen in Fig. 4-4.

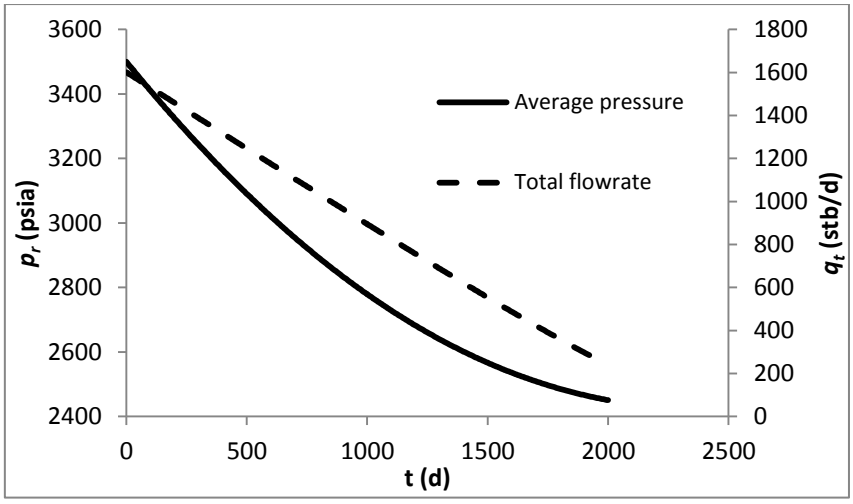

Fig. 4-4 - Pressure and oil's flowrate evolution.

Pressure can also be evaluated considering both its changes with time and distance from the well. An example of pressure behaviour inside a reservoir above the bubble point is shown in Fig. 4-5. The pressure profile's shape is evident throughout the reservoir, and so is the pressure drop with time, considering that the radius zero is the centre of the production well.

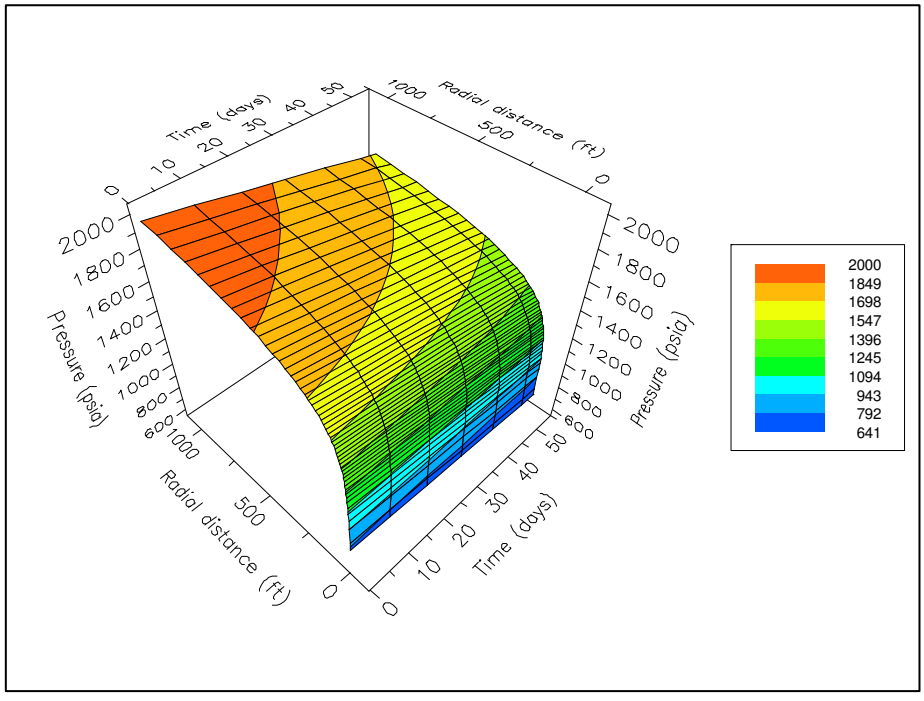

Fig. 4-5 - Pressure evolution in time and with distance from the production well.

The oil's saturation is calculated by a material balance (equation 4-5) which relates the initial oil in the reservoir with the cumulative productions of oil and dissolved-gas N_{go}.

$$S_o = \frac{OOIP - N_o - N_{go}(\rho_g/\rho_o)}{\phi V} \tag{4-5}$$

The cumulative produced dissolved-gas is multiplied by the ratio of the fluids' densities to convert it from volume of gas to the correspondent volume of oil in which it is dissolved.

The water solubility is obtained by applying the principle that the sum of all of the fluids' volume in the reservoir is equal to the pore volume (equation 4-6).

$$1 = S_o + S_w \tag{4-6}$$

Once pressure reaches the bubble point, solution-gas starts evolving from solution. This division point is characterized by evaluating the average reservoir pressure; however, some regions of the reservoir may have already dropped below the bubble point before the considered moment.

This new stage can also be divided into two periods: below and above the critical gas saturation S_{gc}, which determines the moment when gas starts to flow.

First, gas comes out of solution but it is unable to flow as its saturation in the reservoir is less than its critical saturation. While gas is accumulated in the reservoir, pressure drops slowly, improving oil's production.

For the reservoir pressure evaluation not only the oil and dissolved gas produced need to be considered, but also the gas evolved from the solution. The volume of gas in the reservoir G is calculated by the material balance in equation 4-7.

$$G = OOIP \times R_{si} - (OOIP - N_o)R_s - N_{go} \tag{4-7}$$

Where $OOIP$ is the original oil in place, R_{si} and R_s are the initial and current dissolved-gas oil ratio, respectively.

Thus, this expression says that the volume of free gas in the reservoir is the difference between the initial dissolved-gas and the current and produced dissolved-gas.

When gas is formed, volume of oil is reduced, and this volume reduction ΔN is given by equation 4-8, considering that the gas' mass is conserved.

$$G \times \rho_g = \Delta N \times \rho_o \tag{4-8}$$

As a result, the average reservoir pressure variations is now expressed by equation 4-9, which considers the cumulative formation of gas.

$$\overline{p_R} = \overline{p_{R_i}} - \frac{N_o + N_w + N_{go}B_g - GB_g\left(\frac{\rho_o - \rho_g}{\rho_o}\right)}{c_t \phi V} \tag{4-9}$$

As soon as gas saturation exceeds the critical saturation, gas is able to flow and it is produced with oil.

The oil's flowrate in saturated reservoir conditions is estimated by equation 4-10, the gas flowrate by equation 4-11 and finally the water flowrate by equation 4-12 (Beggs 2003, Craft and Hawkins 1991).

$$q_o = \frac{0.00708 k_o h}{(2\overline{p_R})\mu_o B_o[\ln(r_e/r_w)-0.75]}\left(\overline{p_R}^2 - {p_{wf}}^2\right) \tag{4-10}$$

$$q_g = \frac{0.708 k_g h}{Tz\mu_g[\ln(r_e/r_w)-0.75]}\left(\overline{p_R}^2 - {p_{wf}}^2\right) \tag{4-11}$$

$$q_w = \frac{0.00708 k_w h}{(2\overline{p_R})\mu_w B_w[\ln(r_e/r_w)-0.75]}\left(\overline{p_R}^2 - {p_{wf}}^2\right) \tag{4-12}$$

In this period, the equation for determining the pressure profile is obtained by summing the three previous equations, and then it is rearranged to calculate pressure in each point of the horizontal flow.

Moreover, the change in reservoir pressure has to consider the cumulative volume of gas leaving the reservoir N_g, which will increase the pressure drop (equation 4-13).

$$\overline{p_R} = \overline{p_{R_i}} - \frac{N_o + N_w + N_{go}B_g + N_g B_g - G B_g\left(\frac{\rho_o - \rho_g}{\rho_o}\right)}{c_t \phi V} \tag{4-13}$$

Whether the critical gas saturation was exceeded or not, the saturations' calculation has to consider the existence of free gas in the reservoir, which means that gas saturation S_g is greater than zero under the bubble point. The oil saturation is now estimated by equation 4-14.

$$S_o = \frac{OOIP - N_o - N_{go}(\rho_g/\rho_o) - G(\rho_g/\rho_o)}{\phi V} \tag{4-14}$$

The water saturation can also be calculated by a material balance, if its production is considered in this stage, and so the gas saturation is estimated by equation 4-15.

$$1 = S_o + S_g + S_w \tag{4-15}$$

Fig. 4-6 shows the evolution of the average reservoir pressure under the considered mechanism, differentiating the pressure's behaviour as production proceeds.

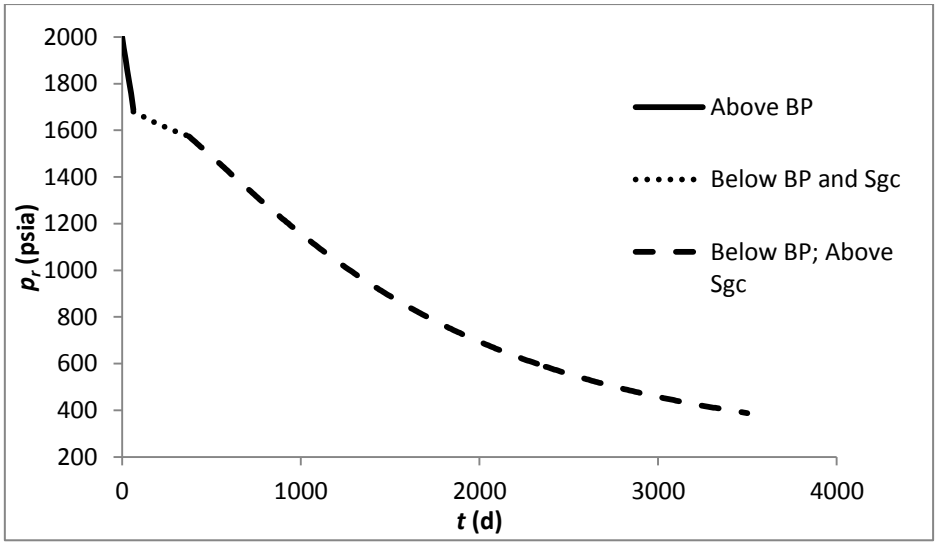

Fig. 4-6 - Evolution of reservoir pressure under a solution-gas drive mechanism.

The calculation of oil's recovery must consider the gas in solution, as it has been proved that a large part of the liquid hydrocarbon produced is obtained from the gas that enters the well. This approach tries to avoid the false assumption that all the free gas entering the well remains in the gaseous phase as it is produced (Cook, Spencer, and Bobrowski 1951).

4.1.2 Piping System

The outflow performance depends on the separator's pressure and on the pressure loss in the well, an illustration of the system is represented in Fig. 4-7. Equation 4-16 represents the application of Bernoulli's equation between the bottom of the well and the separator (Ahmed 2006, Campos 2012).

$$p_{wf} = p_{sep} + \Delta p_f + \Delta p_g \tag{4-16}$$

The friction losses Δp_f are given by equation 4-17, where f is the friction factor, and the gravitational losses Δp_g described by equation 4-18.

$$\Delta p_f = 2\frac{\rho f v^2 L}{g_c D} \tag{4-17}$$

$$\Delta p_g = \frac{\rho g L}{g_c} \tag{4-18}$$

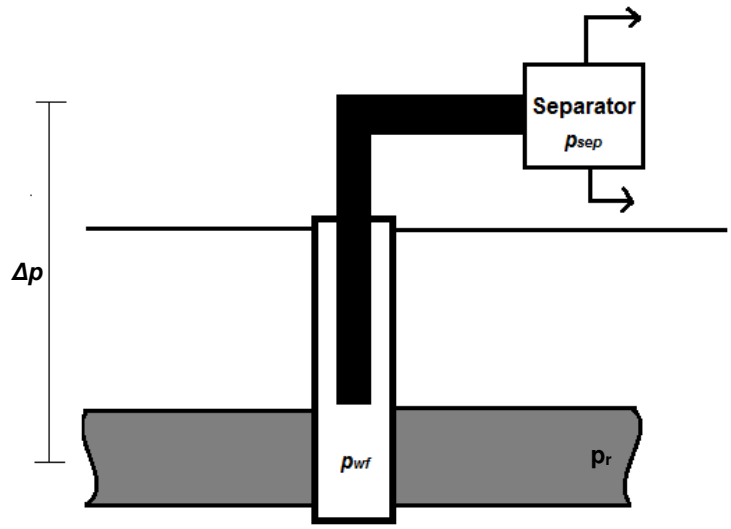

Fig. 4-7 - Illustration of the pressure losses in the piping system from the reservoir to the separator (Beggs 2003).

The density and velocity of the mixture must be evaluated at the well's condition, so it has to be considered that inside the well phase behaviour is altered.

The oil and free gas flowrate entering the separator can be expressed by equations 4-19 and 4-20 respectively, considering the change in gas solubility from the bottom hole to the separator.

$$q_o|_{sep} = q_o|_{wf} B_o - q_o|_{wf} \left(R_s|_{wf} - R_s|_{sep}\right) B_g \frac{\rho_g}{\rho_o} \tag{4-19}$$

$$q_g\big|_{sep} = q_g\big|_{wf} + q_o|_{wf} \left(R_s|_{wf} - R_s|_{sep}\right) B_g \tag{4-20}$$

4.2 Reservoir and Reservoir Fluids' properties

A good prediction of the rock and fluids' properties is vital to correctly estimate the oil production of a reservoir.

4.2.1 Compressibility

Fluids can be divided in incompressible, slightly compressible and compressible. From these categories, the water and oil are considered slightly compressible and gas is compressible. Compressibility calculation can be made using correlation, but for this model it is considered constant for each fluid.

The slightly compressible components have compressibilities of around 10^{-6} $psia^{-1}$, while gas' compressibility varies from 10^{-3} to 10^{-4} $psia^{-1}$, for pressures from 5000 to 500 psia, respectively (IHS 2014).

For the model estimations the total compressibility of the system c_t is required, and it is obtained by equation 4-21, considering that the rock is also slightly compressible.

$$c_t = c_o S_o + c_w S_w + c_g S_g + c_f \tag{4-21}$$

Although all compressibilities are considered constant through time, the total compressibility will suffer changes because of its dependence on fluids' saturation, which change as production progresses (Ahmed 2006, Craft and Hawkins 1991).

4.2.2 Porosity

The assumption that the reservoir rock is slightly compressible determines that the pore volume will suffer alterations during production. This variable can be predicted with equation 4-22 (Ahmed 2006, Craft and Hawkins 1991).

$$\phi = \frac{1}{c_f}\frac{\partial \phi}{\partial p} \tag{4-22}$$

This relationship indicates that when pressure drops, the pore space decreases, decreasing consequently the volume available for fluids' storage.

4.2.3 Permeability

Absolute permeability is crucial to determine the fluids' flow through the porous medium, and, if no data is available, it can be predicted by equation 4-23 (Timur 1968, Ahmed 2006).

$$k = 8.58102 \times 10^3 \frac{\phi^{4.4}}{{S_{wirr}}^2} \tag{4-23}$$

Although absolute permeability is the same for every fluid, their flow is different because it depends on fluids' relative permeability. This type of permeability is calculated based on fluid's saturation.

Moreover, it is important to know the conditions of the reservoir to define what type of relative permeability has to be used. When oil and gas are present, the relative permeabilities can be calculated by equations 4-24 and 4-25, which were proposed by Corey (1954) for gas-displacing oil processes.

$$k_{ro} = \left(1 - \frac{S_g}{1-S_{wirr}}\right)^4 \tag{4-24}$$

$$k_{rg} = \left(\frac{S_g}{1-S_{wirr}}\right)\left(2 - \frac{S_g}{1-S_{wirr}}\right) \tag{4-25}$$

However, the Corey's method is only valid to well-sorted homogenous rocks, and the high dependence of this property on the rock type requires a set of equations which can be used to any type of rock (Ahmed 2006). Table 4-1 shows the different equations for various types of rocks.

Table 4-1- Gas-oil relative permeabilities for various types of reservoir rocks (Ahmed 2006).

Type of reservoir rock	k_{ro}	k_{rg}
Unconsolidated sand, well sorted	$\left(\frac{S_o}{1-S_{wirr}}\right)^3$	$\left(1-\frac{S_o}{1-S_{wirr}}\right)^3$
Unconsolidated sand, poorly sorted	$\left(\frac{S_o}{1-S_{wirr}}\right)^{3.5}$	$\left(1-\frac{S_o}{1-S_{wirr}}\right)^2\left(1-\left(\frac{S_o}{1-S_{wirr}}\right)^{1.5}\right)$
Cemented sandstone, oolitic limestone, rocks with vulgar porosity	$\left(\frac{S_o}{1-S_{wirr}}\right)^4$	$\left(1-\frac{S_o}{1-S_{wirr}}\right)^2\left(1-\left(\frac{S_o}{1-S_{wirr}}\right)^2\right)$

For a successful estimation of oil's production, it is important that these equations are available in the model, so that they can be used based on the type of reservoir that is being studied.

On the other hand, if gas does not exist, and there is water in the reservoir, oil and water relative permeabilities are estimated by the equations in Table 4-2, depending on the type of reservoir rock.

Table 4-2 - Oil-water relative permeabilities for various types of reservoir rocks (Ahmed 2006).

Type of reservoir rock	k_{ro}	k_{rw}
Unconsolidated sand, well sorted	$\left(1-\frac{S_w-S_{wirr}}{1-S_{wirr}}\right)$	$\left(\frac{S_w-S_{wirr}}{1-S_{wirr}}\right)^3$
Unconsolidated sand, poorly sorted	$\left(1-\frac{S_w-S_{wirr}}{1-S_{wirr}}\right)^2\left[1-\left(\frac{S_w-S_{wirr}}{1-S_{wirr}}\right)^{1.5}\right]$	$\left(\frac{S_o}{1-S_{wirr}}\right)^{3.5}$
Cemented sandstone, oolitic limestone, rocks with vulgar porosity	$\left(1-\frac{S_w-S_{wirr}}{1-S_{wirr}}\right)^2\left[1-\left(\frac{S_w-S_{wirr}}{1-S_{wirr}}\right)^2\right]$	$\left(\frac{S_o}{1-S_{wirr}}\right)^4$

These relationships point out that as a fluid is produced, and its saturation in the reservoir decreases, its relative permeability decreases too. When the saturation reaches the irreducible value, the fluid's relative permeability is zero and so the fluid is trapped in the pores due to surface tensions' effect.

4.2.4 Density

The oil density has to be corrected during the life of a reservoir due to pressure decline during oil's production. This correction can be made based on the definition of oil compressibility, equation 4-26 (Ahmed 2006, Craft and Hawkins 1991).

$$\rho_o = \rho_{o\_bp} e^{c_o(p-p_{bp})} \tag{4-26}$$

Where ρ_{o_bp} is the oil density at the bubble point pressure p_{bp}.

However, this relation is just valid for under saturated conditions, because if pressure drops below the bubble point, dissolved-gas comes out of solution, forming free gas. In this case, equation 4-27 is used to predict the changes in the oil's density below the bubble point pressure.

$$\rho_o = \frac{62.4\gamma_o + 0.0136\gamma_g R_s}{B_o} \tag{4-27}$$

This equation includes the oil formation volume factor B_o and specific gravity γ_o, but the most important to note is the presence of the gas specific gravity γ_g and dissolved-gas oil ratio R_s which account for the variations of gas in the solution (Ahmed 2006, Velarde, Blasingame, and W.D. McCain , Beggs 2003).

Above the bubble point the oil's density decreases due to the fact of being slightly compressible. On the other hand, when below the bubble point the density increases as gas comes out of the solution.

The gas density can be calculated by the real-gas equation (equation 4-28), as previously mentioned, by using the definition of gas specific gravity (Ahmed 2006, Beggs 2003).

$$\rho_g = \frac{2.7\gamma_g\overline{p_R}}{(T+460)} \tag{4-28}$$

Equation 4-29 represents the water density estimation based on the density at standard conditions, ρ_{ws} (Chen 2007).

$$\rho_w = \frac{\rho_{ws}}{B_{wi}}\left(1 + c_w\left(\overline{p_R} - \overline{p_{R_i}}\right)\right) \tag{4-29}$$

Where B_{wi} is the initial water formation volume factor.

4.2.5 Viscosity

When the oil is under saturated, its viscosity can be predicted by equation 4-30, which was introduced by Khan et al. (1987).

$$\mu_o = \mu_{o_{bp}}\left(\frac{p}{p_{bp}}\right)^x \tag{4-30}$$

Where $x = 2.6p^{1.187\exp\left(-11.513-8.98\times10^{-5}p\right)}$.

Below the bubble point, the previous equation does not apply and it is replaced by equation 4-31 (Ahmed 2006).

$$\mu_o = \mu_{ob}\left(\frac{p}{p_b}\right)^{-0.14} e^{-2.5\times10^{-4}(p-p_b)} \tag{4-31}$$

For the gas, the Lee-Gonzalez-Eakin Method is applied (equation 4-32), where M_g is the apparent gas molecular weight (Ahmed 2006).

$$\mu_g = \frac{(9.4+0.02M_g)T^{1.5}}{209+19M_g+T}10^{-4}\exp\left[\left(3.5 + 0.01M_g + \frac{986}{T}\right)\left(\frac{\rho_g\times0.0433}{2.7}\right)^{2.4-0.2\left(3.5+0.01M_g+\frac{986}{T}\right)}\right] \tag{4-32}$$

The water viscosity is estimated by considering only temperature effects, which means that it will be constant, as the reservoir temperature is considered constant during production (Chen 2007). Equation 4-33 was introduced by Brill and Beggs (1978).

$$\mu_w = \exp(1.003 - 1.479\times10^{-2}T + 1.982\times10^{-5}T^2) \tag{4-33}$$

4.2.6 Formation Volume Factors

While for pressures above the bubble point the oil formation volume factor can be corrected by the same relation used for density, when pressure drops below this point Standing's correlation is applied (equation 4-34) (Ahmed 2006, Beggs 2003).

$$B_o = 0.9759 + 0.00012\left[R_s\left(\left(\frac{\gamma_g}{\gamma_o}\right)^{1/2} + 1.25T\right)^{1.2}\right] \quad (4\text{-}34)$$

For the gas, the definition of formation volume factor introduced can be applied, and its calculation is based on the volume obtained by the real-gas equation (equation 4-35) (Ahmed 2006, Beggs 2003).

$$B_g = \frac{0.02827zT}{\overline{p_R}} \quad (4\text{-}35)$$

Water formation volume factor is estimated by equation 4-36 (Ahmed 2006).

$$B_w = A_1 + A_2 p + A_3 p^2 \quad (4\text{-}36)$$

Where $A_i = a_1 + a_2(T - 460) + a_3(T - 460)^2$, and the values to complete these equations are represented on Table 4-3.

Table 4-3 - Parameters for the estimation of water formation volume factor (Ahmed 2006).

A_i	a_1	a_2	a_3
A_1	0.9911	$6.35\text{x}10^{-5}$	$8.5\text{x}10^{-7}$
A_2	$-1.093\text{x}10^{-6}$	$-3.497\text{x}10^{-9}$	$4.57\text{x}10^{-12}$
A_3	$-5.0\text{x}10^{-11}$	$6.429\text{x}10^{-13}$	$-1.43\text{x}10^{-15}$

4.2.7 Dissolved-gas oil ratio

The estimation of this variable is made by the use of correlations and its choice will depend on the reservoir production conditions. For this model, the correlation implemented was the one introduced by Al-Marhoun (1988), represented by equation 4-37 (Al-Marhoun 1988, Ahmed 2006).

$$R_s = \left[185.843208{\gamma_g}^{1.877840}{\gamma_o}^{-3.1437}(T + 460)^{-1.32657}\overline{p_R}\right]^{1.39844} \quad (4\text{-}37)$$

However, its use is not always reliable. Therefore, the use of data is advised for the prediction of this property, as it will reduce the errors (Zamani et al. 2015).

The dissolved-gas oil ratio is constant until the bubble point pressure is reached. After this point it declines as reservoir pressure continues to decrease (see Fig. 4-8) (Craft and Hawkins 1991).

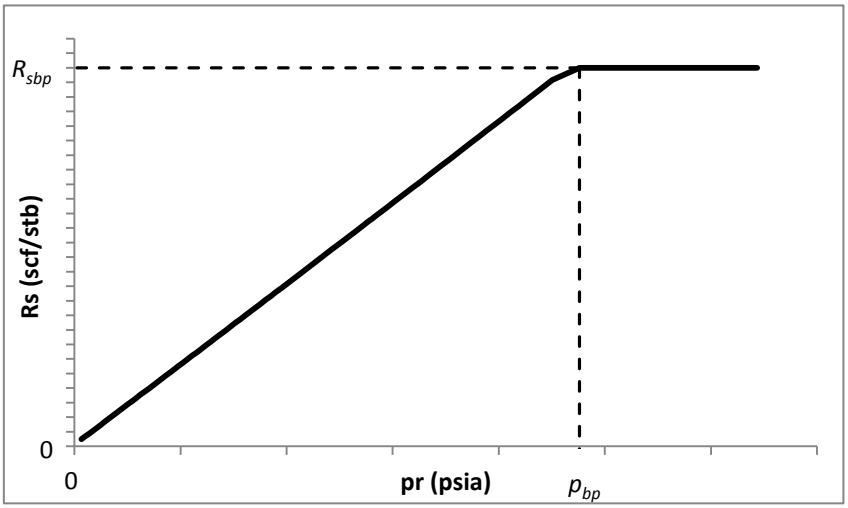

Fig. 4-8 - Dissolved-gas oil ratio vs pressure (Ahmed 2006).

4.2.8 Gas solubility in water

Gas may also be dissolved in water, for this reason equation 4-38 is used to predict this property during production process.

$$R_{sw} = A + B + Cp^2 \tag{4-38}$$

Where $A = 2.12 + 3.45 \times 10^{-3}T(°\text{F}) - 3.59 \times 10^{-5}T^2$; $B = 0.0107 - 5.26 \times 10^{-5}T + 1.48 \times 10^{-7}T^2$; $C = 8.75 \times 10^{-7} + 3.9 \times 10^{-9}T - 1.02 \times 10^{-11}T^2$.

Although this estimation is available, most of the times this value is negligible when compared with the solution-gas oil ratio and for this reason it is assumed zero (Ahmed 2006).

4.2.9 Gas compressibility factor

The gas compressibility factor is an important factor to evaluate the real gas behaviour during the life of the reservoir. Because of the complexibility of its prediction, it is assumed constant in the simulations, and its value is based on the data collected.

4.2.10 Friction factor

The calculation of oil's flowrate relies on the losses in the production well, which depend upon the friction losses. These losses are a function of the friction factor, which is a complex parameter to estimate.

For this reason it is assumed the fixed value of 0.1 for this factor during the life of the reservoir and well.

5 Model Validation and Sensitivity Analysis

The implementation of the equations, presented on the last chapter, on gPROMS® ModelBuilder must be evaluated to understand if the model is capable of correctly predict the oil production of a reservoir with a solution-gas drive mechanism.

The model validation was realized by its application to two different reservoirs: an idealized reservoir and the Louisiana volatile-oil reservoir.

5.1 Idealized Reservoir

Table 5-1 represents the main reservoir properties, and the full description is in Table A-1, Appendix A. In addition to this information it was assumed that the type of rock is a well sorted unconsolidated sand, the gas compressibility factor as 1.06, a friction factor of 0.1 and the gas specific gravity as 1.05.

Table 5-1 - Main idealized reservoir property data (SPE 2015).

Parameter	Value
A (acre)	80
L (ft)	6700
k (mD)	5.0
h (ft)	20
ϕ_i (%)	31
T (°F)	131
$\overline{p_{R_i}}$ (psia)	2000
p_{bp} (psia)	1688
p_{wf} (psia)	199
$OOIP$ (million stb)	2.10
R_{si} (scf/stb)	838.5

This reservoir was idealized to capture the main characteristics and to establish the concept of solution-gas drive. The production data, used to validate the proposed model, are a result of a simulation with a commercial simulator (SPE 2015).

Two approaches were used with the objective of evaluating the correlations' accuracy, while validating the model equations: the use of the property data (Prediction 1) and the use of correlations to calculate the fluids' properties (Prediction 2).

The properties' estimation using the given data was conducted by plotting each property against pressure, and fitting curves to the data points (see Fig A-1 to Fig. A-5) (SPE 2015).

Table 5-2 shows the obtained results for each Prediction of oil formation volume factor and its deviations compared to the data. The equations used in Prediction 1 were equation 5-1 for above the bubble point pressures, and equation 5-2 for pressures below the bubble point.

$$B_o = -3 \times 10^{-5}\overline{p_R} + 1.5198 \tag{5-1}$$

$$B_o = 0.0002\overline{p_R} + 1.1061 \tag{5-2}$$

Above the bubble point the correlation exhibited less deviation, but the results were higher than the data, contrasting with the results of Prediction 1, which were lower than the data.

Below the bubble point, Prediction 1 showed the lowest deviations for higher pressures, but from 1000 to 600 psia Prediction 2 was more accurate.

From an overall perspective, both predictions had acceptable results, as the maximum deviation was in each case near 2% at 1640 psia.

Table 5-2 - Comparison of oil formation volume factor results.

$\overline{p_R}$ (psia)	B_o (bbl/stb)	Pred. 1 Equations (5-1),(5-2)	Deviation	Pred. 2 Equation (4-34)	Deviation
2000	**1.467**	1.460	0.49%	1.470	-0.23%
1700	**1.475**	1.469	0.40%	1.475	0.00%
1640	**1.463**	1.434	1.97%	1.493	-2.03%
1600	**1.453**	1.426	1.84%	1.482	-1.98%
1400	**1.408**	1.386	1.55%	1.429	-1.49%
1200	**1.359**	1.346	0.95%	1.377	-1.33%
1000	**1.322**	1.306	1.20%	1.326	-0.29%
800	**1.278**	1.266	0.93%	1.276	0.14%
600	**1.237**	1.226	0.87%	1.228	0.73%

The oil's viscosity results, Table 5-3, demonstrate that the use of equation 5-3 for pressures above the bubble point results on deviations of around 2%, which is an acceptable value. Equation 5-4, obtained from the data points below the bubble point, is not a good approximation of the fitted data; consequently deviations greater than 13% are observed for pressures higher than 1400 psia.

$$\mu_o = 4 \times 10^{-5} \overline{p_R} + 0.2334 \quad (5\text{-}3)$$

$$\mu_o = 5 \times 10^{-8} \overline{p_R}^{\,2} - 0.0003 \overline{p_R} + 0.6161 \quad (5\text{-}4)$$

On the other hand, the use of correlations appears to be a good property's estimation for the two production stages, achieving the highest deviation of 2.04% at 1200 psia.

Table 5-3 - Comparison of oil viscosity results.

$\overline{p_R}$ (psia)	μ_o (cP)	Pred. 1 Equations (5-3),(5-4)	Deviation	Pred. 2 Equations (4-30),(4-31)	Deviation
2000	0.3201	0.3134	2.09%	0.3166	1.09%
1700	0.3071	0.3009	2.01%	0.3072	-0.03%
1640	0.3123	0.2585	17.23%	0.3120	0.10%
1600	0.3169	0.2640	16.69%	0.3163	0.19%
1400	0.3407	0.2940	13.70%	0.3387	0.58%
1200	0.3714	0.3281	11.66%	0.3638	2.04%
1000	0.3973	0.3660	7.87%	0.3925	1.20%
800	0.4329	0.4081	5.73%	0.4257	1.65%
600	0.4712	0.4540	3.65%	0.4659	1.13%

The gas formation volume factor dependence on pressure according to the data is described by equation 5-5.

$$B_g = 3.249 \overline{p_R} - 1.001 \quad (5\text{-}5)$$

Table 5-4 - Comparison of gas formation volume factor results.

$\overline{p_R}$ (psia)	B_g (bbl/Mscf)	Pred. 1 Equation (5-5)	Deviation	Pred. 2 Equation (4-35)	Deviation
2000	-	-	-	-	-
1700	-	-	-	-	-
1640	1.92	1.97	-2.38%	1.92	-0.13%
1600	1.98	2.01	-1.92%	1.97	0.28%
1400	2.31	2.30	0.21%	2.25	2.43%
1200	2.73	2.69	1.53%	2.63	3.77%
1000	3.33	3.23	3.07%	3.16	5.19%
800	4.16	4.03	3.09%	3.94	5.26%
600	5.47	5.38	1.73%	5.26	3.94%

This relationship shows to be a good approximation of the considered property once Table 5-4 is analysed. When correlation's results are matched with the same obtained

from equation 5-5, it is evident that the use of correlations only induced better results for pressures between 1600 and 1640 psia.

Gas viscosity's prediction through equation 5-6 (Pred. 1) revealed to be advantageous for pressures lower than 1400 psia.

Although deviations for pressures near 1600 psia were greater than 5%, the error decreased with pressure, leading to better results than Pred. 2 as the error in the latter was generally around 4%, excluding 1400 psia (see Table 5-5).

$$\mu_g = 1 \times 10^{-9}\overline{p_R}^2 + 5 \times 10^{-7}\overline{p_R} + 0.0113 \quad (5\text{-}6)$$

Table 5-5 - Comparison of gas viscosity results.

$\overline{p_R}$ (psia)	μ_g (cP)	Pred. 1 Equation (5-6)	Deviation	Pred. 2 Equation (4-32)	Deviation
2000	-	-	-	-	-
1700	-	-	-	-	-
1640	0.0157	0.0148	5.66%	0.0151	4.05%
1600	0.0155	0.0147	5.40%	0.0149	3.96%
1400	0.0140	0.0140	0.28%	0.0141	-0.48%
1200	0.0138	0.0133	3.33%	0.0133	3.46%
1000	0.0132	0.0128	3.02%	0.0126	4.18%
800	0.0126	0.0123	2.06%	0.0120	4.38%
600	0.0121	0.0120	1.15%	0.0115	4.80%

Finally, for the estimation of gas-oil solubility, the implemented correlation (equation 4-37) showed a great disability to do a successful estimation, as seen in Table 5-6.

The deviations of the predicted values increase as pressure decreases showing only acceptable values from 1400 to 1640 psia. However, just a deviation of around 4% in this property leads to greater volume of free gas than in reality, and the reservoir pressure's prediction is compromised in a way that it goes above the bubble point again. Consequently, the simulation crashes at this point.

Table 5-6 – Evaluation of the estimation of gas-oil solubility using equation 4-37.

$\overline{p_R}$ (psia)	R_s (scf/stb)	Prediction Equation (4-37)	Deviation
2000	838.5		
1800	838.5		
1700	838.5		
1640	816.1	782.2	4.2%
1600	798.4	755.7	5.4%
1400	713.4	626.9	12.1%
1200	621.0	505.4	18.6%
1000	548.0	391.6	28.5%
800	464.0	286.6	38.2%
600	383.9	191.7	50.1%

Thus, the same equation (equation 5-7) was used in both predictions.

$$R_s = 0.4158\overline{p_R} + 131.2 \quad (5\text{-}7)$$

The small differences, between the two predictions, detected in Table 5-7 are a result of the other properties' estimation effect on reservoir pressure. It is possible to say this effect is almost negligible when the deviations in both cases are compared.

Table 5-7 – Comparison of dissolved gas oil ratio results.

$\overline{p_R}$ (psia)	R_s (scf/stb)	Pred. 1 Equation (5-7)	Deviation	Pred. 2 Equation (5-7)	Deviation
2000	838.5	838.5	-	838.5	-
1700	838.5	838.5	-	838.5	-
1640	816.1	813.4	0.33%	813.4	0.33%
1600	798.4	796.7	0.21%	796.4	0.25%
1400	713.4	713.5	-0.01%	713.6	-0.03%
1200	621.0	630.2	-1.48%	630.4	-1.52%
1000	548.0	547.1	0.16%	546.9	0.21%
800	464.0	463.8	0.03%	463.7	0.06%
600	383.9	380.9	0.79%	380.7	0.82%

The evolution of gas solubility and cumulative evolved gas obtained in Prediction 1 are represented on Fig. 5-1. As it was expected, while solubility decreases, the volume of free gas increases.

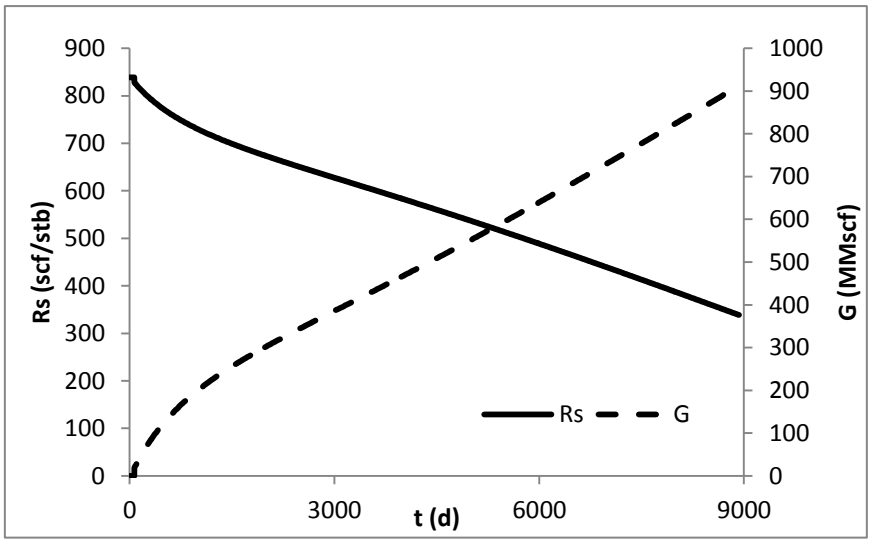

Fig. 5-1 - Results of prediction 1 results for the gas solubility and cumulative free gas.

5.1.1 Evaluation of oil production

After analysing the properties, the oil's production must be studied. Fig 5-2 illustrates the reservoir pressure evolution against the cumulative oil produced for the two predictions and the idealized curve. Table A-2 represents the plotted results and data.

The two predicted curves are almost coincident, which indicates that the differences commented above do not have a great impact on the reservoir performance estimation, and so the use of correlations can be assumed accurate.

Although the predicted curves seem to follow the correct pattern, for a given pressure the predicted oil produced is lower than the idealized quantity, and this difference increases as pressure decreases in the reservoir.

One of the reasons for this difference at lower pressures is the fact that the idealized curve considered oil production until 0 psia was reached in the reservoir. This is an impossible pressure to reach, and so Fig. 5-2 only considers production until 500 psia, which is when, according to the executed simulation, the residual oil saturation is reached, and oil production stops.

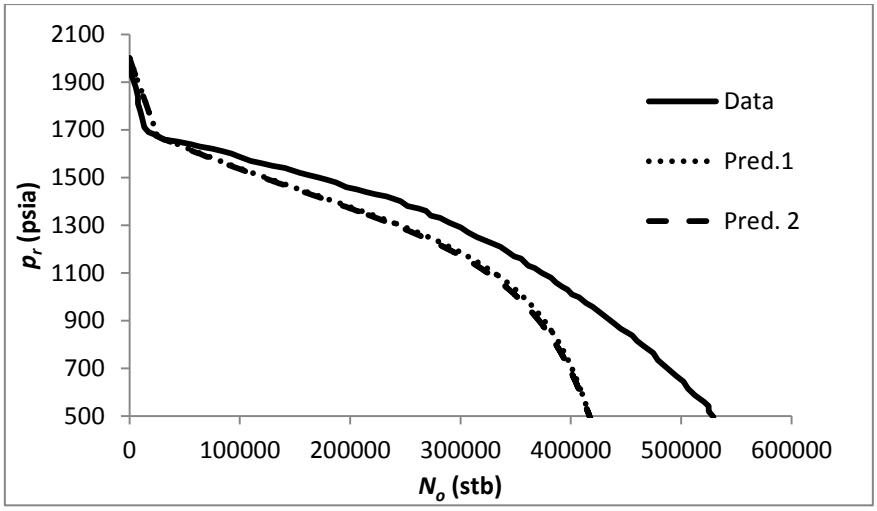

Fig. 5-2 – Comparison of the two production curves predicted with the data.

Besides that fact, the estimation of oil production may be affected by any miscalculation of saturation or relative permeability, whose evolutions with time are represented in Fig. 5-3 and Fig. 5-4. The absence of information on relative permeability of the fluids' requires the use of correlations for the assumed type of rock.

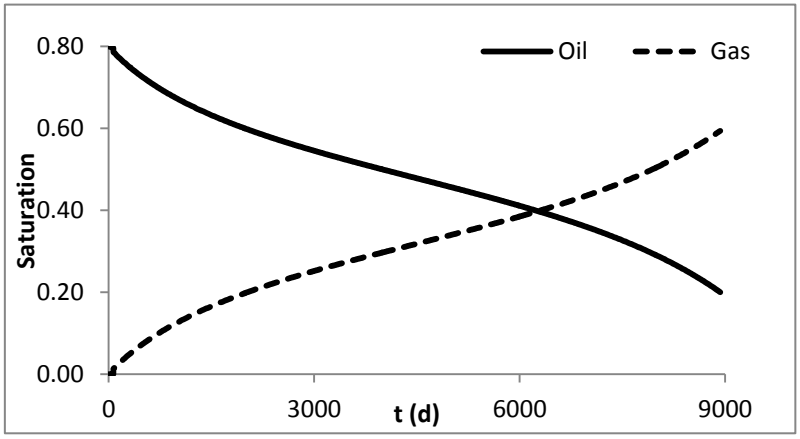

Fig. 5-3 – Results of Prediction 1 for the oil and gas saturations.

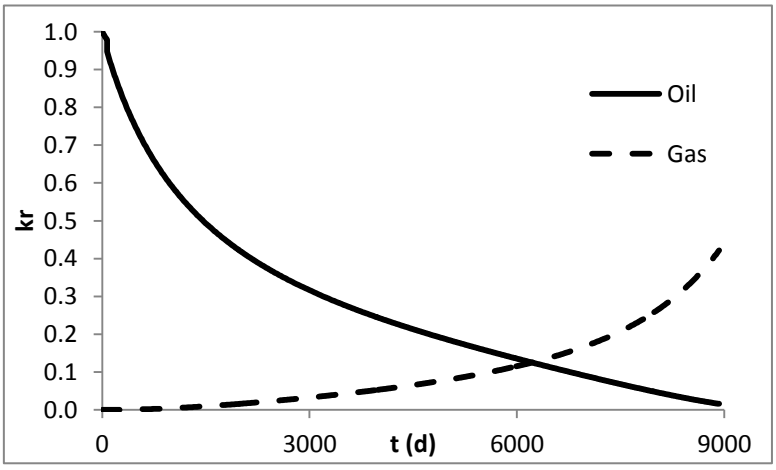

Fig. 5-4 – Results for the relative permeabilities of oil and gas, Prediction 1.

Also, the assumption that the flow is horizontal and that the flowrates inside the reservoir are constant may have an important role in the observed deviations of the prediction of oil's production, especially when gas exists in the reservoir.

Fig. 5-5 illustrates the pressure variation with time and radius obtained from prediction 1. Recalling that the radius zero corresponds to the centre of the production well, the pressure profile inside the reservoir is perceptible from the plot. When evaluating pressure with time, this plot shows that the pressure at each point of the reservoir decreases with time.

As the wellbore flowing pressure was fixed at 199 psia, this is the pressure for the radius zero for all the production time.

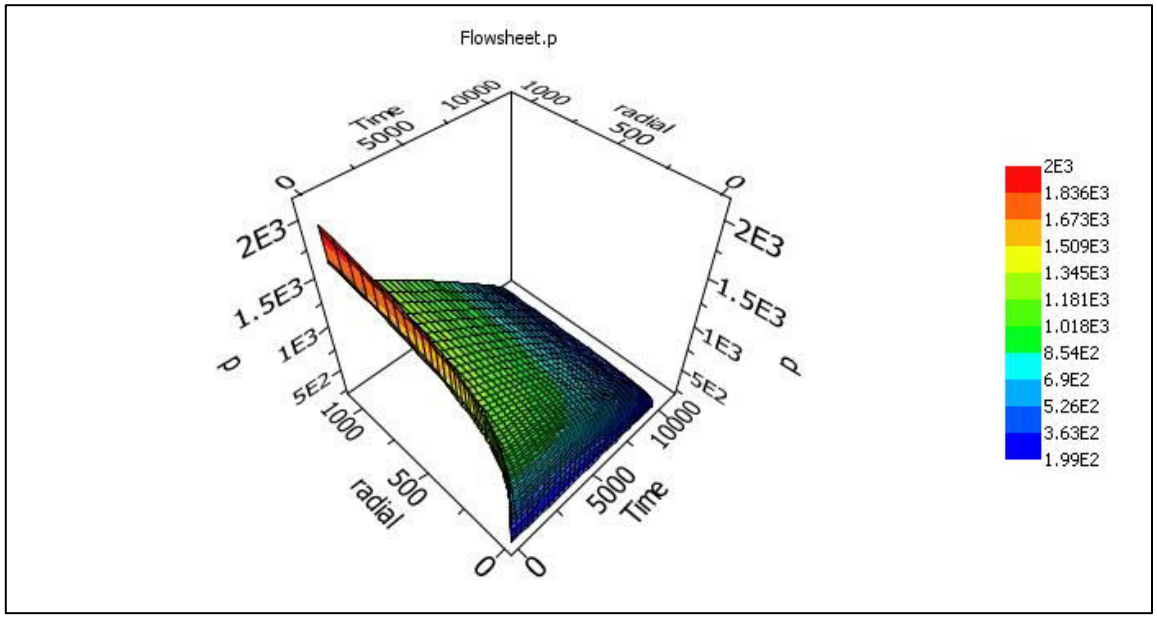

Fig. 5-5 - Simulation output of the pressure variation with time and radius obtained from Prediction 1.

5.2 Louisiana volatile-oil reservoir

The reservoir was discovered in 1953 in North Louisiana, and on August 1956 it was completely developed with 11 wells. The most important reservoir properties and initial conditions are in Table 5-8, and the complete list is in Table B-1, Appendix B (Jacoby and V. J. Berry 1957, Cordell and Ebert 1965, SPE 2015).

Table 5-8 - Main reservoir properties (Jacoby and V. J. Berry 1957, Cordell and Ebert 1965, SPE 2015).

Parameter	Value
$\overline{p_{R_i}}$ (psia)	5070
p_{bp} (psia)	4698
p_{sep} (psia)	500
L (ft)	10000
T (°F)	246
R_{si} (scf/stb)	2909
$OOIP$ (million stb)	10.992
k (mD)	174
h (ft)	24.4
ϕ_i (%)	13.6
A (acre)	1568

These properties were implemented in the simulation, in addition to the fluids' property data presented on Fig. B-1 to Fig. B-5. Despite of the existence of 11 wells, this fact was not considered and the simulation only reflected the production of one well for the same total drainage area of the reservoir.

The fitted curves of the different fluids' properties against reservoir pressure were used to calculate the oil and gas formation volume factors, viscosity and also the dissolved-gas oil ratio, when the reservoir was saturated. Above the bubble point, the relations implemented in the model were applied because of the lack of confidence in the fitted curves based on the data, especially in the case of the oil formation volume factor (see Fig. B-1).

Table 5-9 shows the results of oil formation volume factor and viscosity and its deviations. The equations used for these calculations were equation 5-8 and equation 5-9, respectively.

$$B_o = 1.4 \times 10^{-14}\overline{p_R}^4 - 1 \times 10^{-10}\overline{p_R}^3 + 4 \times 10^{-7}\overline{p_R}^2 - 0.0003\overline{p_R} + 1.2924 \quad (5\text{-}8)$$

$$\mu_o = 0.3685\exp(-3 \times 10^{-4}\overline{p_R}) \quad (5\text{-}9)$$

It is clear that the fitted curve for the formation volume factor is not a good approximation mostly for high pressures, generating deviations from the real value greater than 26%.

The viscosity estimation has acceptable deviations, achieving its maximum value of 16.3% at 4398 psia. However, it is important to note that a tendency exists on the estimation of both properties, as deviation decreases with pressure.

This indicates that during the life of the reservoir, such changes occur on the fluid´s behaviour that it justifies the use of different equations in different periods.

Another conclusion that may be made by the analysis of Table 5-9 is that the deviation is always a negative number, which indicates that the equations overestimate the properties' value.

Table 5-9 – Results' evaluation of oil formation volume factor and viscosity.

$\overline{p_R}$ (psia)	B_o (bbl/stb)	Prediction Equation (5-8)	Deviation	μ_o (cP)	Prediction Equation (5-9)	Deviation
5070	2.704	2.744	-1.5%	0.0742	0.0729	1.8%
4998	2.713	2.746	0.0%	0.0735	0.0724	1.5%
4798	2.740	2.751	0.0%	0.0716	0.0712	0.6%
4698	2.754	2.754	0.0%	0.0706	0.0706	0.0%
4398	2.338	2.945	-26.0%	0.0847	0.0985	-16.3%
4198	2.204	2.793	-26.7%	0.0906	0.1045	-15.3%
3998	2.093	2.653	-26.8%	0.0968	0.1110	-14.6%
3798	1.991	2.526	-26.9%	0.1028	0.1179	-14.7%
3598	1.905	2.411	-26.6%	0.1104	0.1251	-13.3%
3398	1.828	2.302	-25.9%	0.1177	0.1329	-12.9%
3198	1.758	2.202	-25.2%	0.1242	0.1410	-13.5%
2998	1.686	2.102	-24.7%	0.1325	0.1499	-13.1%
2798	1.632	2.008	-23.0%	0.1409	0.1591	-12.9%
2598	1.580	1.916	-21.3%	0.1501	0.1689	-12.5%
2398	1.534	1.824	-18.9%	0.1598	0.1796	-12.4%
2198	1.490	1.737	-16.6%	0.1697	0.1906	-12.3%
1998	1.450	1.652	-13.9%	0.1817	0.2024	-11.4%
1798	1.413	1.569	-11.0%	0.1940	0.2150	-10.8%
1598	1.367	1.491	-9.1%	0.2064	0.2283	-10.6%
1398	1.333	1.420	-6.5%	0.2223	0.2422	-9.0%
1198	1.305	1.355	-3.8%	0.2438	0.2574	-5.6%
998	1.272	1.302	-2.4%	0.2629	0.2731	-3.9%
798	1.239	1.261	-1.8%	0.2882	0.2900	-0.6%

Above the bubble point, the observed deviations for both properties are smaller than 2%, which points out that the relations presented on section 4 of this monography describe correctly the oil's behaviour.

The calculation of the same properties for the gas, using equations 5-10 and 5-11, is analysed in Table 5-10.

$$B_g = 1.5531\overline{p_R}^{(-0.899)} \tag{5-10}$$

$$\mu_g = 1 \times 10^{-9}\overline{p_R}^2 - 1 \times 10^{-6}\overline{p_R} + 0.0143 \tag{5-11}$$

Table 5-10 -Results' evaluation of gas formation volume factor and viscosity.

$\overline{p_R}$ (psia)	B_g (bbl/Mscf)	Prediction Equation (5-10)	Deviation	μ_g (cP)	Prediction Equation (5-11)	Deviation
5070	-	-	-	-	-	-
4998	-	-	-	-	-	-
4798	-	-	-	-	-	-
4698	-	-	-	-	-	-
4398	0.853	0.824	3.4%	0.0350	0.0293	16.4%
4198	0.874	0.858	1.8%	0.0327	0.0278	15.1%
3998	0.901	0.897	0.4%	0.0306	0.0263	14.0%
3798	0.933	0.940	-0.7%	0.0288	0.0249	13.4%
3598	0.970	0.986	-1.7%	0.0271	0.0237	12.7%
3398	1.015	1.039	-2.3%	0.0255	0.0225	11.9%
3198	1.066	1.096	-2.8%	0.0240	0.0214	11.0%
2998	1.125	1.163	-3.4%	0.0227	0.0203	10.6%
2798	1.196	1.236	-3.4%	0.0214	0.0193	9.6%
2598	1.281	1.321	-3.1%	0.0203	0.0185	9.0%
2398	1.380	1.422	-3.1%	0.0193	0.0176	8.6%
2198	1.498	1.538	-2.6%	0.0184	0.0169	8.0%
1998	1.642	1.675	-2.0%	0.0175	0.0163	6.9%
1798	1.819	1.843	-1.3%	0.0168	0.0157	6.4%
1598	2.035	2.050	-0.7%	0.0161	0.0153	5.3%
1398	2.315	2.308	0.3%	0.0155	0.0149	4.1%
1198	2.689	2.656	1.2%	0.0150	0.0145	3.1%
998	3.190	3.124	2.1%	0.0146	0.0143	2.1%
798	3.911	3.819	2.4%	0.0142	0.0141	0.4%

The curve fitted for the formation volume factor describes successfully its evolution as pressure decreases, since the maximum deviation observed was 3.4%. It is important to

mention that the predicted values are smaller than the expected ones for higher (3998-4398 psia) and lower (798-1398 psia) pressures, but they are greater between this two ranges, i.e. from 1598 to 3798 psia.

For the gas viscosity's case, it is observed that the deviation of the estimated values decreases as pressure drops, and the maximum deviation obtained was 16.4% at 4398 psia. In this case, every estimated value is lower than the expected.

In Appendix C, a suggestion to decrease the deviations in the prediction of oil formation volume factor and oil and gas viscosity is presented.

Last but not least it is necessary to study the evolution of dissolved-gas oil ratio, which is discretised in Table 5-11 and Table 5-12.

$$R_s = 197.21\exp(0.0006\overline{p_R}) \tag{5-12}$$

The equation used for its prediction (equation 5-12) does not expect a decrease as high as the data implied for the higher pressures. Between 4398 and 3798 psia the deviations range from -22.9% to -16.8%, which indicate that the equation for this pressure interval should be altered for a better estimate. The predicted values are greater than the real ones until pressure reaches 2398 psia, and from this pressure until 1198 psia the prediction is smaller than reality. However, from this point on, the prediction is again higher than the data.

Table 5-11 - Results' evaluation of dissolved-gas oil ratio.

$\overline{p_R}$ (psia)	R_s (scf/stb)	Prediction Equation (4-37)	Deviation
5070	2909	2909	-
4998	2909	2909	-
4798	2909	2909	-
4698	2909	2909	-
4398	2247	2762	-22.9%
4198	2019	2454	-21.5%
3998	1828	2175	-19.0%
3798	1651	1928	-16.8%
3598	1500	1711	-14.1%
3398	1364	1516	-11.1%
3198	1237	1347	-8.9%
2998	1111	1192	-7.3%
2798	1013	1058	-4.5%

Table 5-12 – (continuing) Results' evaluation of dissolved-gas oil ratio.

$\overline{p_R}$ (psia)	R_s (scf/stb)	Prediction Equation (4-37)	Deviation
2598	918	939	-2.3%
2398	833	831	0.3%
2198	752	737	2.0%
1998	677	654	3.4%
1798	608	579	4.7%
1598	524	514	2.0%
1398	461	456	1.0%
1198	406	404	0.4%
998	344	359	-4.4%
798	283	318	-12.5%

5.2.1 Evaluation of oil production

After the properties' analyses, one should revise the predicted oil production, and compare it with the real results. Fig. 5-6 shows the cumulative oil produced with pressure progress, and the plotted values are detailed in Table B-2.

The effect of gas solubility's miscalculation is clear in Fig. 5-6, as an unexpected pressure drop happens after the bubble point pressure is achieved. However, the predicted curve has the correct tendency, since pressure maintenance leads to higher recoveries, and when gas production starts, the rate of oil production decreases.

After about 3000 psia, the predicted curve does not describe the same curvature as the data curve; instead it is nearly a straight line. This phenomenon can be explained by the combination of all the assumptions made in the model.

These assumptions may not be fully correct when a large quantity of gas forms in the reservoir, because reservoir characteristics start to be more similar to a gas reservoir than to a liquid's reservoir (Woods 1935).

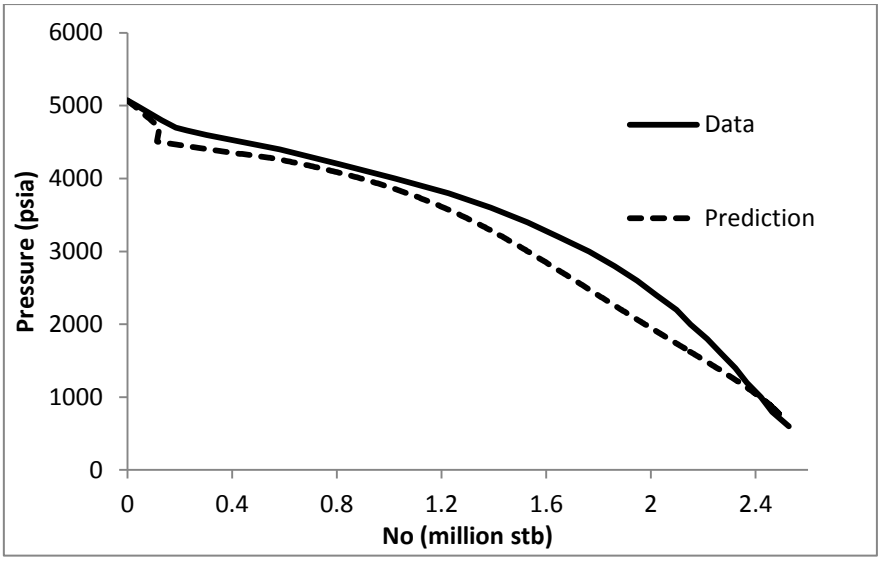

Fig. 5-6 – Comparison of actual performance with model prediction of pressure evolution with oil production.

For a deeper analysis, one can study the cumulative gas evolved from solution and solubility, whose evolutions are represented in Fig. B-6, and Fig. 5-7 shows the period worth studying.

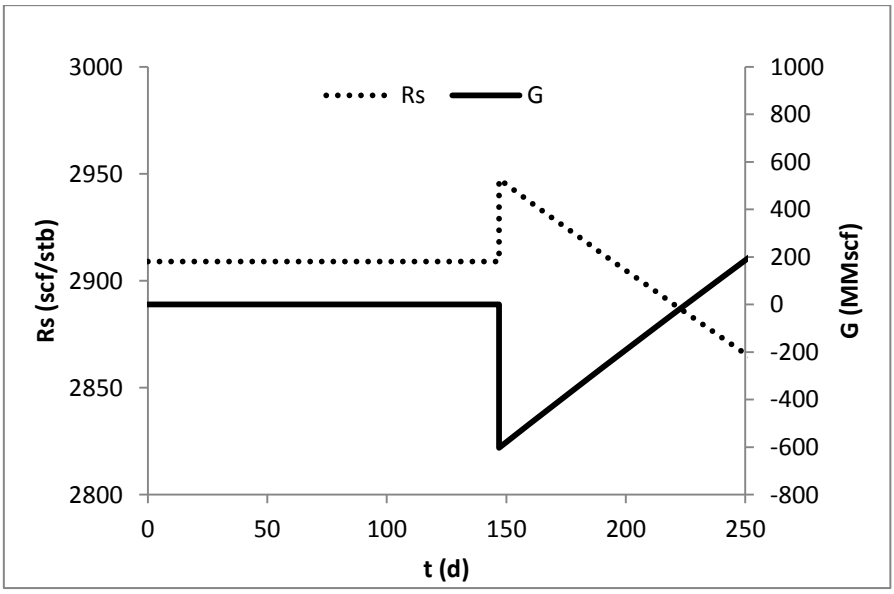

Fig. 5-7 – Prediction of cumulative volume of free gas evolution with time.

In the beginning of the production, there is no free gas in the reservoir and gas solubility is constant; when reservoir pressure reaches the bubble point, gas evolves from solution, as gas solubility drops. Contrarily, the simulation's results showed in Fig. 5-7 denote an increase in solubility, leading to negative values of cumulative volume of free gas in the reservoir.

As a result, the model predicts ineffectively the reduction in pressure, which explains the excessive pressure drop, the moment bubble point pressure is reached. Instead of a

positive value, which would contribute to reservoir pressure maintenance, the cumulative free gas is negative, resulting from the solubility increase and the nonexistence of free gas in the reservoir.

Fig. 5-8 shows the variation of oil and gas flowrate with time. When pressure is greater than the bubble point, there is no gas flowrate, and the oil flowrate decreases. As soon as this pressure is achieved, due to pressure decrease, a sudden decrease is observed in the oil flowrate, but as pressure is maintained by the evolved gas, oil flowrate increases.

The moment gas saturation exceeds the critical one, gas flowrate increases until it reaches its maximum. In this stage the oil flowrate decreases quickly because of the higher mobility of gas, which allows it to flow better through the porous medium.

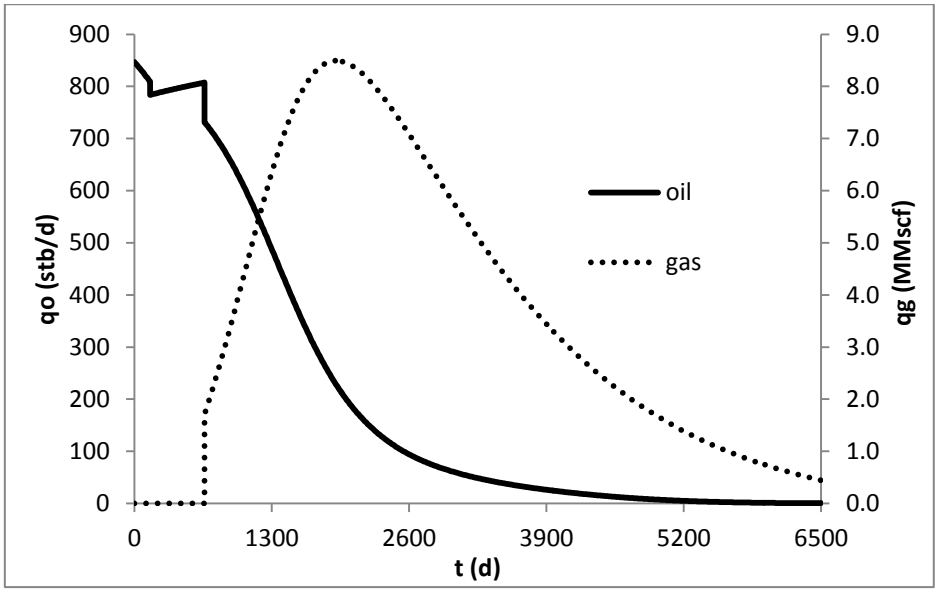

Fig. 5-8 - Predicted oil and gas flowrate vs time.

Fig. 5-9 illustrates the oil and gas saturation, and it is noticeable that gas saturation is influenced by the error in the cumulative free gas. However, their general behaviour is correct as oil saturation decreases and gas saturation increases with time.

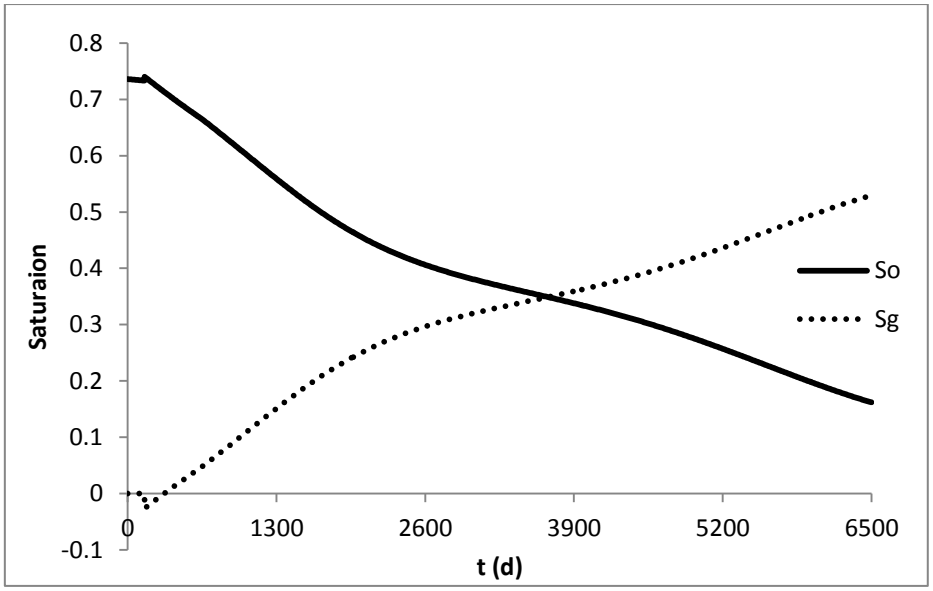

Fig. 5-9 – Oil and gas saturations vs time.

The relative permeabilities of oil and gas are represented in Fig. 5-10, and once again the effect of the miscalculations previously mentioned is noticeable in the gas saturation curve. Because gas saturation is negative, its relative permeability is also negative and consequently the oil's is greater than one.

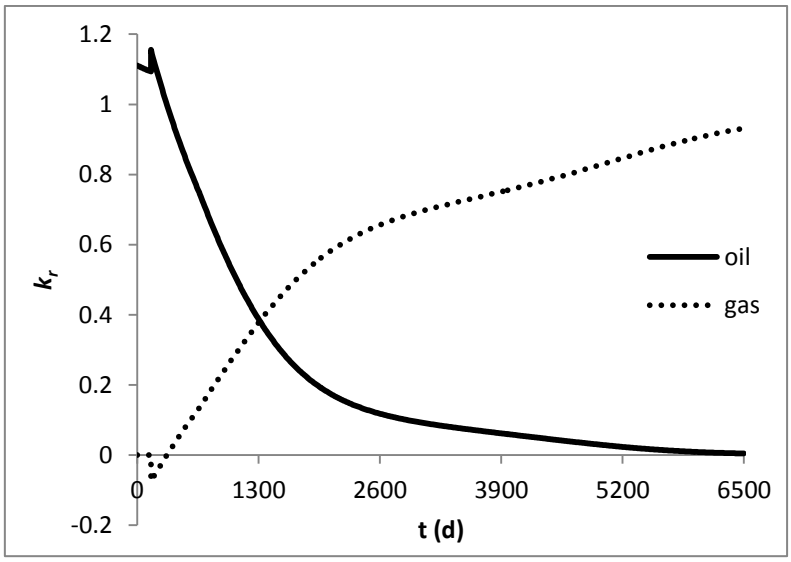

Fig. 5-10 – Oil and gas relative permeabilities vs time.

The pressure evolution based on the time production is represented in Fig. 5-11.The three production stages are correctly represented with greater pressure decline above the bubble point and when gas production starts (4200 psia approximately) than between these periods, which is when gas is accumulated inside the reservoir.

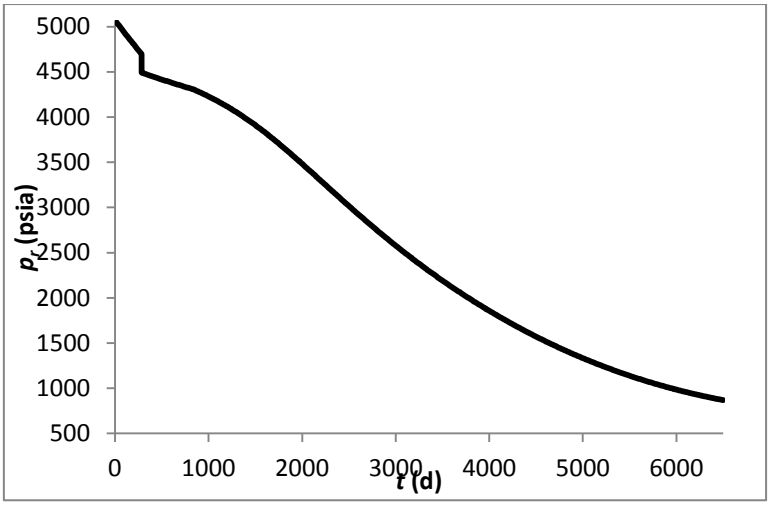

Fig. 5-11 - Average reservoir pressure vs time.

The total time estimated of oil production was of about sixteen years, which is more than the reported time of 12 years, from 1953 until 1965. This can be explained by mainly the fact that the simulation only considered one producing well, while in reality there were eleven wells producing for the same drainage area (Jacoby and V. J. Berry 1957, Cordell and Ebert 1965).

Pressure evolution can also be evaluated based on the radius, Fig 5-12 shows a plot of the pressure variation with time and radius.

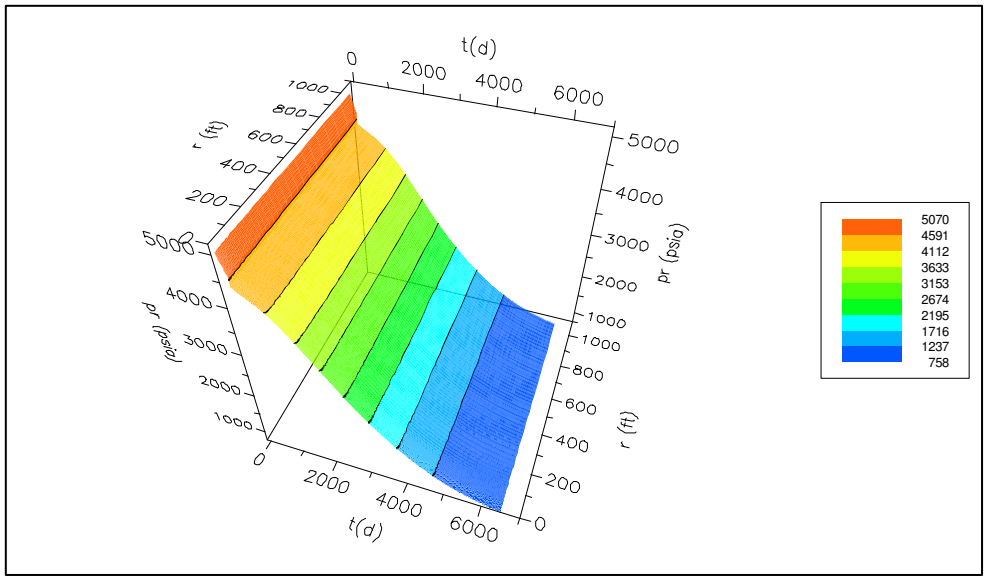

Fig. 5-12 - Pressure variation with time and radius obtained from the simulation.

Although the pressure drop as production progresses is clear in Fig. 5-12, the reservoir pressure profile cannot be commented by the analysis of this plot.

For this reason, pressure should be plotted just against radius, resulting on Fig. 5-13, which shows the reservoir's pressure profile at the beginning and at the end of the production.

The two curves show the expected pattern for a pressure profile and the difference in pressure ranges between them results from the production process.

At the initial moment the pressure inside the reservoir ranges from 5070 to 5033 psia, and after the fluids' production the new pressure range is of 765 to 758 psia.

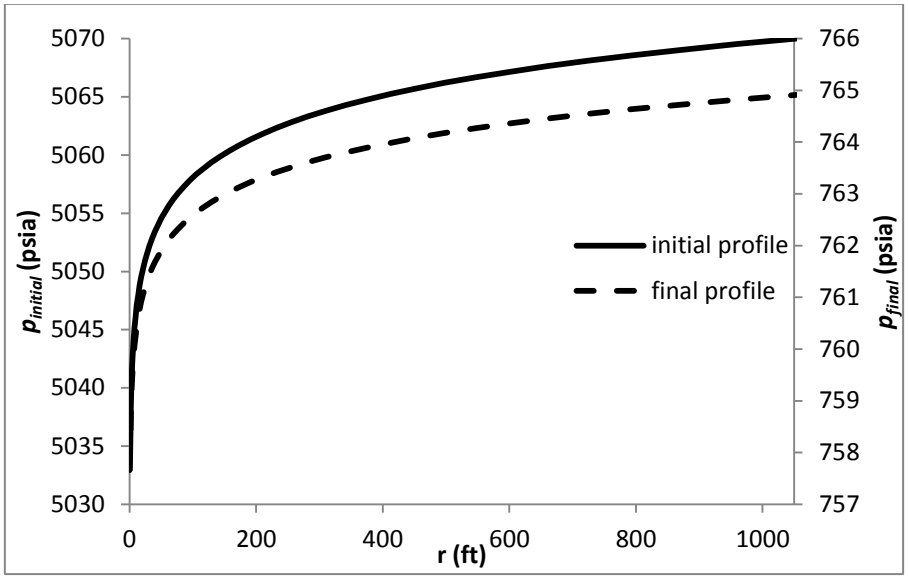

Fig. 5-13 - Initial and final pressure profile of the simulated reservoir.

6 Conclusion and Future Work

The Nodal Analysis showed to be a good method for predicting oil's production, despite all the assumptions and simplifications made. However, better techniques of properties' estimation should be considered to improve the results' quality, mainly when pressures start to drop to low values.

For the correct prediction of the recovered oil, from a reservoir containing highly volatile oil, it is essential to include the dissolved-gas that may be recovered. The assumption that all the evolved gas that enters the well stays in the gaseous phase can lead to inaccuracies in the results.

The results of model verification indicate that the gas' behaviour, especially for low pressures, may have a great effect on oil's flow and recovery, damaging the curve of average reservoir pressure against cumulative produced oil. For this matter, it should be considered that the reservoir starts to behave more similarly to a gas reservoir.

The errors observed for lower pressures may not be too problematic in real practice, because near the bubble point pressure it is recommended to initiate secondary or enhanced oil recovery to maintain pressure and consequently improve oil's production.

In the future, correlations for the gas compressibility factor and the friction factor should be included in the model. In the case of the friction factor, it is even possible to eliminate the outflow performance equations and connect the reservoir model to a well model, which will result in better predictions.

7 References

Ahmed, Tarek. 2006. *Reservoir Engineering Handbook*. 3rd ed: Elsevier Inc.

Al-Marhoun, M. A. 1988. "PVT Correlations for Middle East Crude Oils." *Journal of Petroleum Technology* no. 40:650-666.

Barker, C., W. K. Robbins, C. S. Hsu, L. J. Drew, and and Updated by Staff. 2005. Petroleum. In *Kirk-Othmer Encyclopedia of Chemical Technology*.

Beggs, H. Dale. 2003. *Production Optimization using NODAL™ Analysis*. 2nd ed. Tulsa, Oklahoma: OGCI and Petroskills Publications.

Brill, J., and H. Beggs. 1978. Two-Phase Flow in Pipes. The University of Tulsa.

Campos, João Moreira de. 2012. *Notas Para o Estudo de Mecânica dos Fluidos*: Departamento de Engenharia Química da Faculdade de Engenharia da Universidade do Porto.

Chen, Zhangxin. 2007. *Reservoir Simulation - Mathematical tecniques in Oil Recovery*: Society for Industrial and Applied Mathematics.

Cook, Alton B., G. V. Spencer, and F. P. Bobrowski. 1951. "Special Considerations in predicting reservoir performance of highly volatile type oil reservoirs." *Petroleum Transactions, AIME* no. 192.

Cordell, J. C., and C. K. Ebert. 1965. "A Case History Comparison of Predicted and Actual Performance of a Reservoir Producing Volatile Crude Oil." *Journal of Petroleum Technology* no. 11.

Corey, A. T. 1954. "The interrelation between gas and oil relative permeabilities." *Producers Monthly* no. 19:38-41.

Craft, B. C., and M. Hawkins. 1991. *Applied Petroleum Reservoir Engineering*. 2nd ed.

Dake, L. P. 1978. *Fundamentals of reservoir engineering*. 1st ed, *Developments in Petroleum Science*: ELSEVIER SCIENCE B.V.

David Martin, F., and Robert M. Colpitts. 1996. "5 - Reservoir Engineering." In *Standard Handbook of Petroleum and Natural Gas Engineering*, edited by William C. Lyons, 1-362. Houston: Gulf Professional Publishing.

Hocking, Martin B. 2005. "18 - Petroleum Refining." In *Handbook of Chemical Technology and Pollution Control (Third Edition)*, edited by Martin B. Hocking, 593-636. San Diego: Academic Press.

IHS. *Reservoir Properties* 2014 [cited May 11th 2015. Available from http://www.fekete.com/SAN/WebHelp/FeketeHarmony/Harmony_WebHelp/Content/HTML_Files/Reference_Material/General_Concepts/Reservoir_Properties.htm.

Jacoby, R. H., and Jr. V. J. Berry. 1957. "A Method for Predicting Depletion Performance of a Reservoir Producing Volatile Crude Oil." *Petroleum Transactions, AIME* no. 210.

Khan, S.A., M.A. Al-Marhoun, and S.A. Abu-Khamsin. 1987. Viscosity Correlations for Saudi Arabian Crude Oils. SPE Paper No. 15720.

Levorsen, A. I. 1956. *Geology of petroleum*: W. H. Freeman.

Metz, Bert, Ogunlade Davidson, Heleen Coninck, Manuela Loos, and Leo Meyer. 2005. *Carbon Dioxide Capture and Storage*: Cambridge Universsity Press.

PSE. *The Advanced Process Modelling company* [cited June 22nd 2015. Available from http://www.psenterprise.com/company.html.

PSE. *gPROMS ModelBuilder* [cited June 23rd 2015. Available from http://www.psenterprise.com/modelbuilder.html.

PSE. *New gCCS system modelling technology used for Shell Peterhead project* 2014a [cited June 22nd 2015. Available from http://www.psenterprise.com/news/press_releases/140731_shell_peterhead/index.html.

PSE. *PSE launches gCCS - world's first full-chain modelling software for CCS* 2014b [cited June 22nd 2015. Available from http://www.psenterprise.com/news/press_releases/140710_gccs/index.html.

Reinicke, K. M., G. Hueni, N. Liermann, J. Oppelt, P. Reichetseder, and W. Unverhaun. 2014. Oil and Gas, 6. Reservoir Performance. In *Ullman's Encyclopedia of Industrial Chemistry*.

SPE. 2015. *Solution gas drive reservoirs*. SPE, June 3rd 2015 2015 [cited May 24th 2015]. Available from http://petrowiki.org/Solution_gas_drive_reservoirs.

Sureshjani, Mohammadhossein Heidari, and Shahab Gerami. 2011. "An analytical model for production data analysis of under saturated oil reservoirs." *Journal of Petroleum Science and Engineering* no. 78:23-31.

Timur, A. 1968. "An Investigation Of Permeability, Porosity, & Residual Water Saturation Relationships For Sandstone Reservoirs." *The Log Analyst IX* no. 4.

Velarde, J., T. A. Blasingame, and Jr. W.D. McCain. Correlation of Black Oil Properties at Pressures Below Bubble Point Pressure - A New Approach. The Petroleum Society.

Woods, Rex W. 1935. "Case History of Reservoir Performance of a Highly Volatile Type Oil Reservoir." *Petroleum Transactions, AIME* no. 204.

Zamani, Hossein Ali, Shahin Rafiee-Taghanaki, Masoud Karimi, Milad Arabloo, and Abbas Dadashi. 2015. "Implementing ANFIS for prediction of reservoir oil solution gas-oil ratio." *Journal of Natural Gas Science and Engineering* no. 25:325-334.

Appendix A – Idealized Reservoir Data and Results

Table A-1- Idealized reservoir property data (SPE 2015).

Parameter	Value
A (acre)	80
L (ft)	6700
k (mD)	5.0
h (ft)	20
ϕ_i (%)	31
T (°F)	131
$\overline{p_{R_i}}$ (psia)	2000
p_{bp} (psia)	1688
p_{wf} (psia)	199
p_{sep} (psia)	100
$OOIP$ (million stb)	2.10
R_{si} (scf/stb)	838.5
S_{wirr} (%)	20
S_{gc} (%)	5
$S_{or}(\%)$	20
B_{oi} (bbl/stb)	1.466
γ_o	0.85
γ_g	1.06

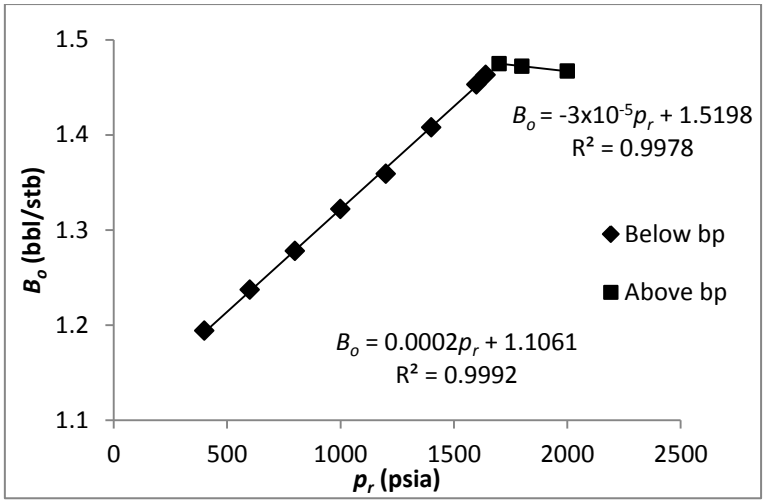

Fig. A-1 - Oil formation volume factor data and fitted curves (SPE 2015).

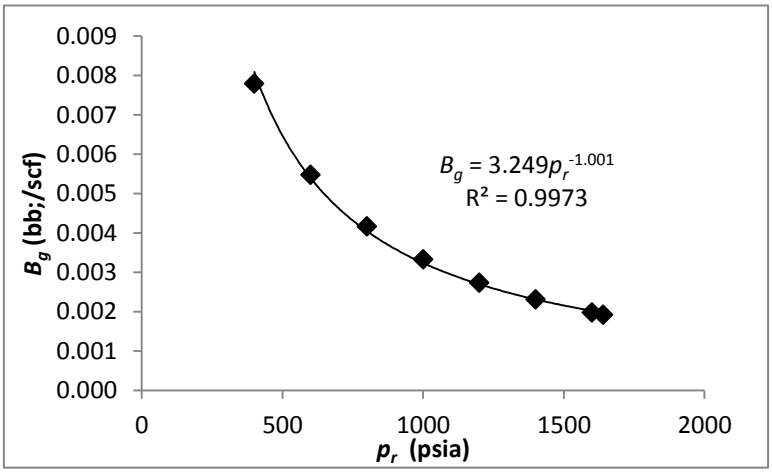

Fig. A-2 - Gas formation volume factor data and fitted curve (SPE 2015).

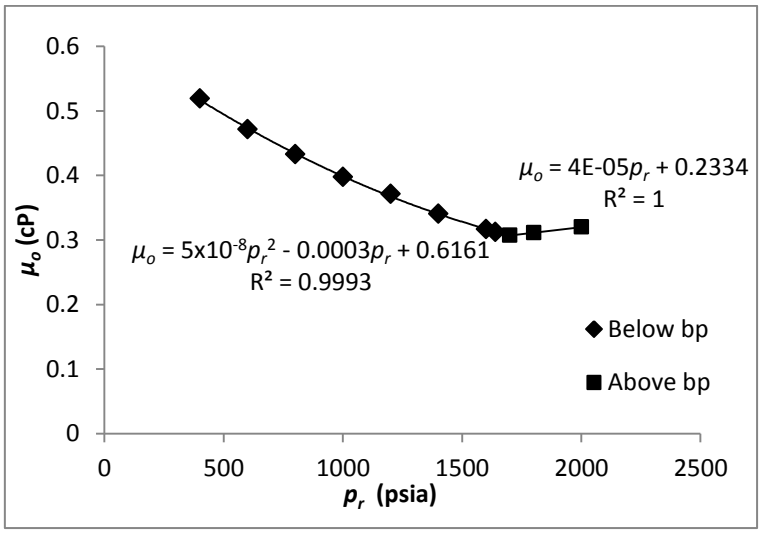

Fig. A-3 - Oil viscosity data and fitted curve (SPE 2015).

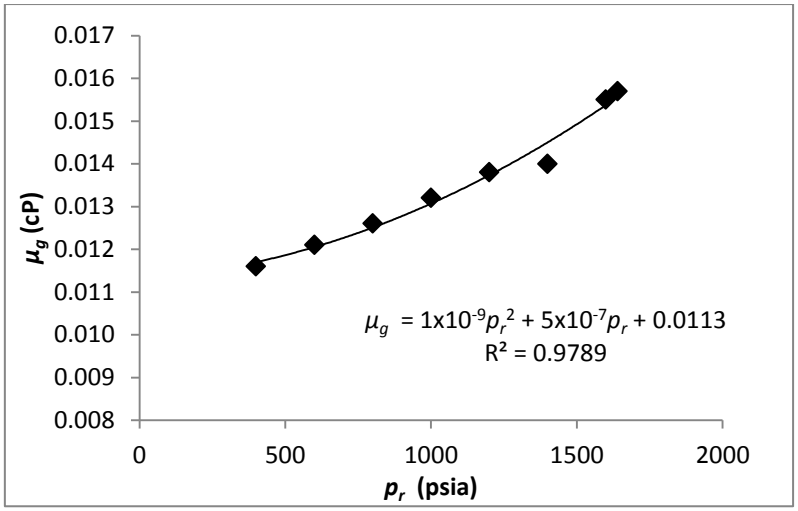

Fig. A-4 - Gas viscosity data and fitted curve (SPE 2015).

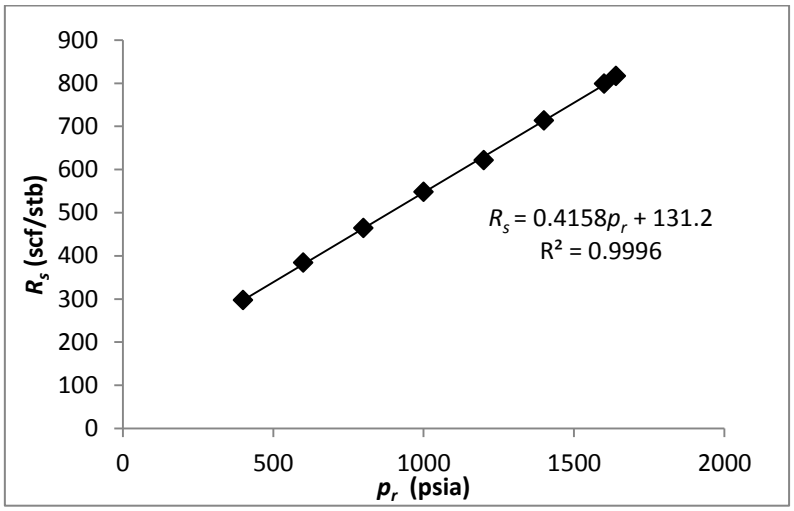

Fig. A-5 - Dissolved-gas oil ratio data (SPE 2015).

Table A-2 – Analysis of the evolution of recovery with pressure.

pr (psia)	Recovery (%)	Pred. 1	Deviation	Pred. 2	Deviation
2000	0.00	0.00	-	0	-
1810	0.37	0.69	-88.0%	0.68	-84.8%
1780	0.46	0.85	-85.5%	0.84	-82.4%
1680	1.10	1.16	-5.5%	1.16	-5.1%
1660	1.47	1.49	-1.1%	1.53	-4.1%
1650	2.11	1.86	11.6%	1.76	16.8%
1640	2.66	2.05	23.0%	1.98	25.7%
1630	3.03	2.32	23.5%	2.26	25.3%
1620	3.58	2.58	27.9%	2.47	30.9%
1610	4.04	2.83	29.8%	2.75	32.0%
1600	4.40	3.08	29.9%	3.01	31.5%
1590	4.68	3.35	28.3%	3.27	30.0%
1570	5.23	3.94	24.6%	3.78	27.8%
1560	5.69	4.24	25.5%	4.08	28.3%
1550	6.15	4.45	27.6%	4.37	28.9%
1540	6.70	4.80	28.4%	4.60	31.4%
1520	7.34	5.33	27.4%	5.20	29.1%
1500	8.17	5.89	27.9%	5.72	30.0%
1450	9.82	7.35	25.2%	7.22	26.5%
1400	11.70	8.86	24.3%	8.66	26.0%
1360	12.80	10.00	21.9%	9.84	23.1%
1310	13.80	11.41	17.3%	11.19	18.9%
1270	14.60	12.44	14.8%	12.21	16.4%
1210	16.00	13.78	13.8%	13.55	15.3%
1160	16.90	14.76	12.7%	14.50	14.2%
1100	17.80	16.99	4.6%	15.46	13.1%
1040	18.70	16.53	11.6%	16.26	13.1%
1010	19.10	16.88	11.6%	16.61	13.0%
974	19.70	17.25	12.4%	16.99	13.8%
912	20.60	17.80	13.6%	17.57	14.7%
866	21.20	18.15	14.4%	17.94	15.4%
815	21.90	18.48	15.6%	18.31	16.4%
764	22.60	18.77	16.9%	18.62	17.6%
701	23.20	19.09	17.7%	18.97	18.2%
615	24.10	19.45	19.3%	19.38	19.6%
519	25.00	19.79	20.8%	19.77	20.9%

Appendix B – Louisiana Volatile-Oil Reservoir Data and Results

Table B-1 – Reservoir property data (Jacoby and V. J. Berry 1957, Cordell and Ebert 1965, SPE 2015).

Parameter	Value
$\overline{p_{R_i}}$ (psia)	5070
p_{bp} (psia)	4698
p_{sep} (psia)	500
L (ft)	10000
T (°F)	246
T_{sep} (°F)	65
R_{si} (scf/stb)	2909
$OOIP$ (million stb)	10.992
k (mD)	174
h (ft)	24.4
ϕ_i (%)	13.6
A (acre)	1568
S_{wirr} (%)	28.3
B_{oi} (bbl/stb)	2.703
γ_o	51.2

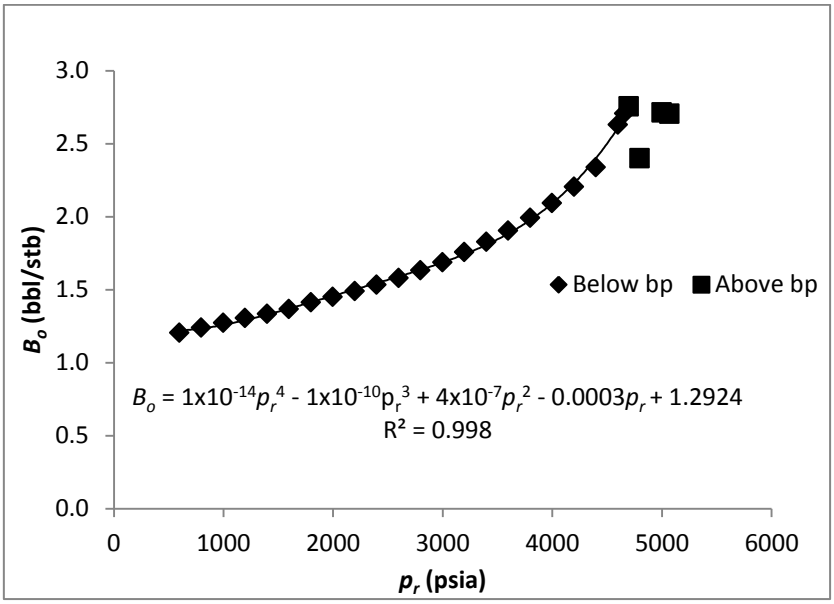

Fig. B-1 – Oil formation volume factor data and fitted curve (SPE 2015).

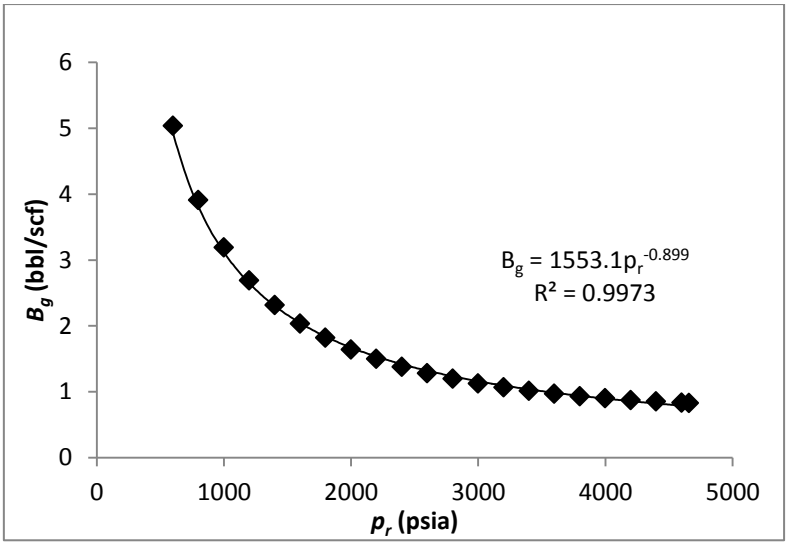

Fig. B-2 - Gas formation volume factor and fitted curve (SPE 2015).

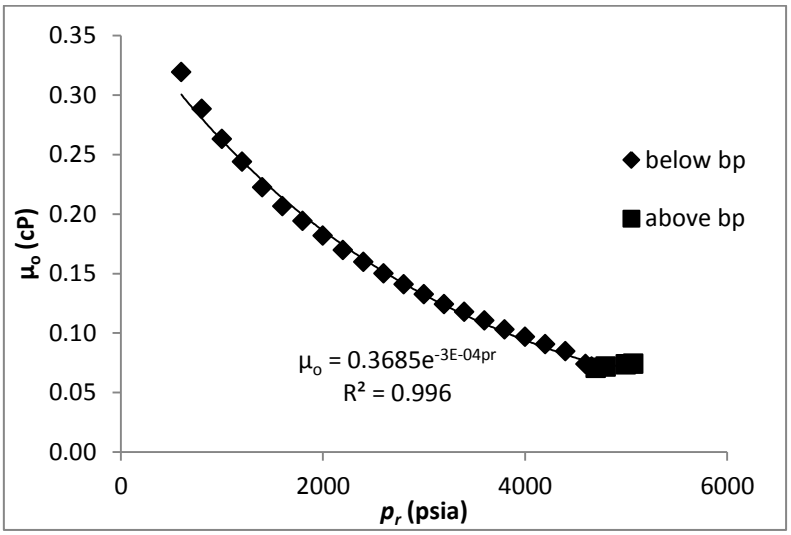

Fig. B-3 - Oil viscosity data and fitted curve (SPE 2015).

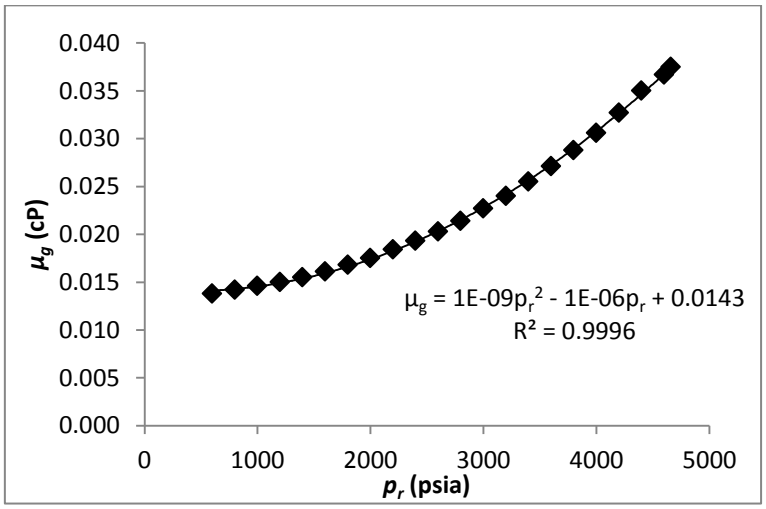

Fig. B-4 - Gas viscosity data and fitted curve (SPE 2015).

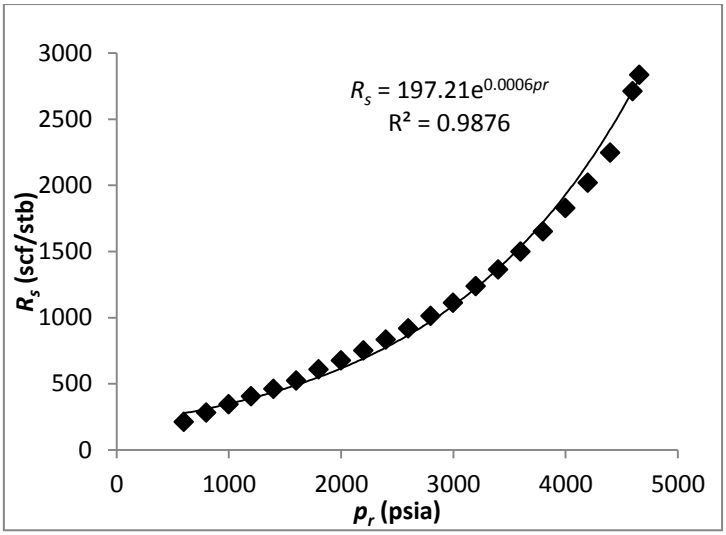

Fig. B-5 - Dissolved-gas oil ratio data (SPE 2015).

Table B-2 - Evolution of cumulative oil production, and results' analysis.

$\overline{p_R}$ (psia)	N_o (million stb)	Predicted	Deviation
5070	0	0	-
4998	0.036	0.025	29.8%
4798	0.130	0.092	29.5%
4698	0.184	0.122	33.9%
4398	0.582	0.311	46.6%
4198	0.808	0.668	17.3%
3998	1.022	0.891	12.8%
3798	1.227	1.255	-2.3%
3598	1.388	1.208	13.0%
3398	1.528	1.328	13.1%
3198	1.646	1.431	13.0%
2998	1.764	1.530	13.3%
2798	1.861	1.621	12.9%
2598	1.947	1.709	12.2%
2398	2.022	1.799	11.0%
2198	2.097	1.888	10.0%
1998	2.151	1.977	8.1%
1798	2.215	2.070	6.6%
1598	2.269	2.162	4.7%
1398	2.323	2.252	3.1%
1198	2.366	2.338	1.2%
998	2.420	2.418	0.1%
798	2.463	2.481	-0.7%

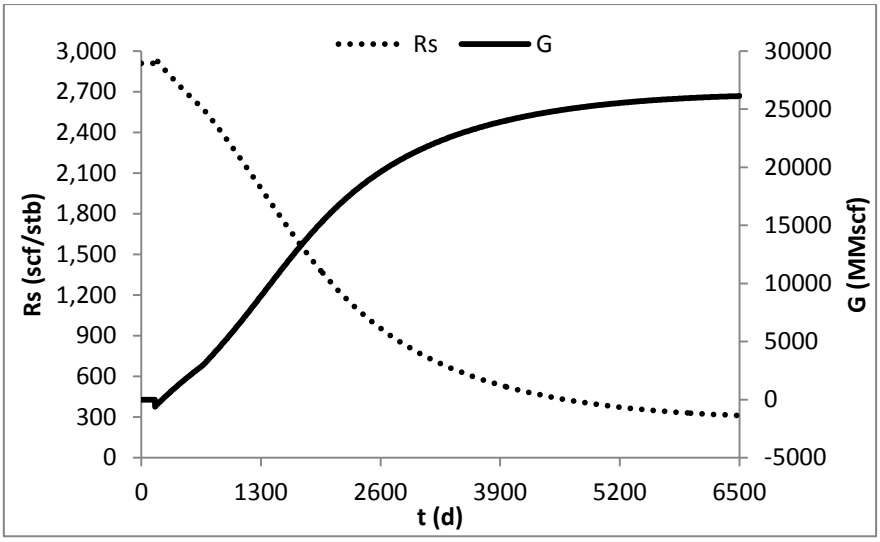

Fig. B-6 – Dissolved-gas oil ratio and cumulative free gas vs time.

Appendix C – Corrections

The properties' prediction of the Louisiana volatile-oil reservoir using the fitted curve to the data showed large deviations. This may be caused by the use of few decimal numbers in the equations' parameters.

Table C-1 relates the results of equation (5-8) with equation (C-1) in the oil formation volume factor calculation.

$$B_o = 1.2223 \times 10^{-14}\overline{p_R}^4 - 9.9170 \times 10^{-11}\overline{p_R}^3 + 3.0764 \times 10^{-7}\overline{p_R}^2 - 2.1697 \times 10^{-4}\overline{p_R} + 1.2574 \quad \text{(C-1)}$$

Table C-1 - Correction of oil formation volume factor.

$\overline{p_R}$ (psia)	B_o (bbl/stb)	Equation (5-8)	Deviation	Equation (C-1)	Deviation
4398	2.338	2.945	-26.0%	2.389	-2.2%
4198	2.204	2.793	-26.7%	2.225	-0.9%
3998	2.093	2.653	-26.8%	2.090	0.1%
3798	1.991	2.526	-26.9%	1.979	0.6%
3598	1.905	2.411	-26.6%	1.888	0.9%
3398	1.828	2.302	-25.9%	1.812	0.9%
3198	1.758	2.202	-25.2%	1.747	0.6%
2998	1.686	2.102	-24.7%	1.690	-0.2%
2798	1.632	2.008	-23.0%	1.638	-0.4%
2598	1.580	1.916	-21.3%	1.590	-0.6%
2398	1.534	1.824	-18.9%	1.543	-0.6%
2198	1.490	1.737	-16.6%	1.498	-0.5%
1998	1.450	1.652	-13.9%	1.453	-0.2%
1798	1.413	1.569	-11.0%	1.409	0.3%
1598	1.367	1.491	-9.1%	1.367	0.0%
1398	1.333	1.420	-6.5%	1.328	0.4%
1198	1.305	1.355	-3.8%	1.293	0.9%
998	1.272	1.302	-2.4%	1.267	0.4%
798	1.239	1.261	-1.8%	2.389	-2.2%

The use of equation (C-1) clearly improved the prediction of this property below the bubble point, decreasing the error to less than 1% in the majority of the pressures considered.

The prediction of oil viscosity was also improved by equation (C-2) and the comparison between equation (C-2) and equation (5-9) is shown in Table C-2.

$$\mu_o = 3.6412 \times 10^{-1} \exp(-3.3524 \times 10^{-4} \overline{p_R}) \quad \text{(C-2)}$$

Table C-2 - Correction of oil viscosity.

$\overline{p_R}$ (psia)	μ_o (cP)	Equation (5-9)	Deviation	Equation (C-2)	Deviation
4398	0.0847	0.0985	-16.3%	0.0834	1.6%
4198	0.0906	0.1045	-15.3%	0.0891	1.6%
3998	0.0968	0.1110	-14.6%	0.0953	1.5%
3798	0.1028	0.1179	-14.7%	0.1019	0.9%
3598	0.1104	0.1251	-13.3%	0.1090	1.3%
3398	0.1177	0.1329	-12.9%	0.1166	1.0%
3198	0.1242	0.1410	-13.5%	0.1246	-0.3%
2998	0.1325	0.1499	-13.1%	0.1333	-0.6%
2798	0.1409	0.1591	-12.9%	0.1425	-1.1%
2598	0.1501	0.1689	-12.5%	0.1524	-1.5%
2398	0.1598	0.1796	-12.4%	0.1630	-2.0%
2198	0.1697	0.1906	-12.3%	0.1743	-2.7%
1998	0.1817	0.2024	-11.4%	0.1864	-2.6%
1798	0.1940	0.2150	-10.8%	0.1993	-2.7%
1598	0.2064	0.2283	-10.6%	0.2131	-3.2%
1398	0.2223	0.2422	-9.0%	0.2279	-2.5%
1198	0.2438	0.2574	-5.6%	0.2437	0.0%
998	0.2629	0.2731	-3.9%	0.2606	0.9%
798	0.2882	0.2900	-0.6%	0.2787	3.3%

At high pressures, the deviations decreased from around 15% to around 1.5%.

The gas viscosity's prediction also showed deviations that implied that the fitted curve was not fully correct. Equation (C-3) is presented as a solution to this miscalculation.

$$\mu_g = 1.2787 \times 10^{-9}\overline{p_R}^2 - 9.8812 \times 10^{-7}\overline{p_R} + 1.4256 \times 10^{-2} \qquad \text{(C-3)}$$

Table C-3 - Correction of gas viscosity.

$\overline{p_R}$ (psia)	μ_g (cP)	Equation (5-11)	Deviation	Equation (C-3)	Deviation
4398	0.0350	0.0293	16.4%	0.0346	1.0%
4198	0.0327	0.0278	15.1%	0.0326	0.2%
3998	0.0306	0.0263	14.0%	0.0307	-0.5%
3798	0.0288	0.0249	13.4%	0.0289	-0.5%
3598	0.0271	0.0237	12.7%	0.0273	-0.6%
3398	0.0255	0.0225	11.9%	0.0257	-0.6%
3198	0.0240	0.0214	11.0%	0.0242	-0.7%
2998	0.0227	0.0203	10.6%	0.0228	-0.4%
2798	0.0214	0.0193	9.6%	0.0215	-0.5%
2598	0.0203	0.0185	9.0%	0.0203	-0.1%
2398	0.0193	0.0176	8.6%	0.0192	0.3%
2198	0.0184	0.0169	8.0%	0.0183	0.8%
1998	0.0175	0.0163	6.9%	0.0174	0.6%
1798	0.0168	0.0157	6.4%	0.0166	1.1%
1598	0.0161	0.0153	5.3%	0.0159	1.0%
1398	0.0155	0.0149	4.1%	0.0154	0.8%
1198	0.0150	0.0145	3.1%	0.0149	0.6%
998	0.0146	0.0143	2.1%	0.0145	0.4%
798	0.0142	0.0141	0.4%	0.0143	-0.6%

This new equation allowed achieving deviations lower than 1% in most of the pressures studied.

This study demonstrates that the errors in the prediction of these three properties were due to the fact that not enough decimal numbers were used in the fitted curves.